Schinke-Nendza, Aiko

Working Paper

Cross-sectoral coordination in highly interconnected multi-operator energy systems - A distributed framework with autonomous agents

HEMF Working Paper, No. 04/2024

Provided in Cooperation with:
University of Duisburg-Essen, Chair for Management Science and Energy Economics

Suggested Citation: Schinke-Nendza, Aiko (2024) : Cross-sectoral coordination in highly interconnected multi-operator energy systems - A distributed framework with autonomous agents, HEMF Working Paper, No. 04/2024, University of Duisburg-Essen, House of Energy Markets & Finance (HEMF), Essen

This Version is available at:
https://hdl.handle.net/10419/307710

Cross-sectoral coordination in highly interconnected multi-operator energy systems – A distributed framework with autonomous agents

HEMF Working Paper No. 04/2024

by

Aiko Schinke-Nendza

July 2024

UNIVERSITÄT
DUISBURG
ESSEN

Open-Minded

Cross-sectoral coordination in highly interconnected multi-operator energy systems – A distributed framework with autonomous agents by Aiko Schinke-Nendza

Abstract

Facing the intertwined challenges in the energy sector of achieving net-zero carbon emissions and integrating renewable energies, there is a pressing need for innovative solutions that are also capable of addressing inefficiencies in existing coordination frameworks. Therefore, this paper proposes a novel distributed framework with autonomous agents to facilitate cross-sectoral coordination of interconnected multi-operator energy systems. The technology-independent framework is applicable to various multi-energy systems and enhances economic transparency and consistency in financial settlements. By introducing pairwise dependencies, the approach restricts information exchange to bilateral communication between physically connected agents, ensuring the autonomy and confidentiality of commercially sensitive and critical infrastructure-related information. Additionally, the framework supports fully distributed and parallel co-optimization of all agents, eliminating the need for centralized coordination and reducing communication steps per iteration. A comprehensive case study focusing on a decarbonized scenario of Germany underscores the framework's tractability and scalability, suggesting its suitability for large-scale applications. Equivalent results to a single-operator framework are obtained, highlighting the framework's potential to offer market-driven incentives for efficient resource allocation. Different indicators for convergence are introduced and assessed regarding the intricacies of the financial settlement process of the framework.

Keywords: OR in energy, cross-sectoral coordination, distributed market-clearing, multi-operator energy systems, autonomous agents

JEL-Classification: C61 (Optimization Techniques), C63 (C63 – Simulation Modeling), Q40 (Energy – General), Q41 (Energy – Demand and Supply;Prices), Q43 (Energy and the Macroeconomy)

AIKO SCHINKE-NENDZA

House of Energy Markets and Finance
University of Duisburg-Essen, Germany
Universitätsstr. 12, 45117 Essen
+49-(0)201 / 183-5625
aiko.schinke-nendza@uni-due.de
www.hemf.wiwi.uni-due.de

Cross-sectoral coordination in highly interconnected multi-operator energy systems – A distributed framework with autonomous agents

Aiko Schinke-Nendza[a]

[a]*House of Energy Markets and Finance, University of Duisburg-Essen, Universitätsstr. 12, 45117, Essen, Germany*

Abstract

Facing the intertwined challenges in the energy sector of achieving net-zero carbon emissions and integrating renewable energies, there is a pressing need for innovative solutions that are also capable of addressing inefficiencies in existing coordination frameworks. Therefore, this paper proposes a novel distributed framework with autonomous agents to facilitate cross-sectoral coordination of interconnected multi-operator energy systems. The technology-independent framework is applicable to various multi-energy systems and enhances economic transparency and consistency in financial settlements. By introducing pairwise dependencies, the approach restricts information exchange to bilateral communication between physically connected agents, ensuring the autonomy and confidentiality of commercially sensitive and critical infrastructure-related information. Additionally, the framework supports fully distributed and parallel co-optimization of all agents, eliminating the need for centralized coordination and reducing communication steps per iteration. A comprehensive case study focusing on a decarbonized scenario of Germany underscores the framework's tractability and scalability, suggesting its suitability for large-scale applications. Equivalent results to a single-operator framework are obtained, highlighting the framework's potential to offer market-driven incentives for efficient resource allocation. Different indicators for convergence are introduced and assessed regarding the intricacies of the financial settlement process of the framework.

Keywords: OR in energy, cross-sectoral coordination, distributed market-clearing, multi-operator energy systems, autonomous agents

Email address: aiko.schinke-nendza@uni-due.de (Aiko Schinke-Nendza)

1. Introduction

Europe has positioned itself at the forefront of the energy transition by its commitment to achieve climate neutrality by 2050, aligning with the Paris Agreement's objectives. This transition necessitates a transformative overhaul of the energy sector, pivotal in reducing greenhouse gas emissions, cf. Bouckaert et al. (2021). Amidst this transformation, energy systems currently face multiple intertwined challenges and opportunities that have to be addressed. For instance, to achieve net-zero carbon emissions, a massive integration of renewable energies and cross-sectoral solutions is required, cf. Jimenez-Navarro et al. (2020). Furthermore, the decentralization of demand and supply, via multiple small-scale units, emphasizes the need for refined market operations that consider the limits of existing infrastructure, cf. Pinson (2023). Here, the ongoing digitalization is expected to enhance the connectivity and optimization capabilities among decentralized units and networks, thus paving the way for innovative coordination mechanisms while promoting new business opportunities, cf. Küfeoglu et al. (2019).

To address these challenges while harnessing digitalization-related benefits, this paper presents a novel distributed coordination framework tailored for cross-sectoral energy markets with multiple network operators. It introduces autonomous agents, i.e., market participants and network operators, that engage in distributed communication with their physically interconnected neighbors exclusively. Employing a fully distributed decomposition-based approach, this framework ensures the confidentiality of sensitive data for both market participants and network operators while maintaining manageable problem sizes for those agents. Furthermore, the economic interpretability and the interoperability are assessed for a large-scale application, which demonstrates the scalability and tractability of the framework.

1.1. Paradigms in existing coordination frameworks

Today's designs of energy systems are based on one of two alternative paradigms: sequential and simultaneous coordination frameworks. For instance, the prevalent electricity market design in Europe is based on a market-clearing followed by a subsequent network operation. While its simplicity has been instrumental for the implementation and promotion, such frameworks are increasingly challenged by increasing inefficiencies, especially with respect to congestion management. Conversely, the US has pioneered electricity market designs that build on simultaneous coordination. While being effective in coordinating market-clearing and network operations based on nodal prices, such frameworks grapple with the fundamental regulatory

requirement regarding information disclosure by market participants. To scrutinize the trade-offs between both frameworks, subsequently, the implementational challenges inherent to both approaches are highlighted.

In Europe, the electricity sector evolved from integrated monopolies and national zonal markets to a coupled European market for electricity, cf. Weber (2023). In this context, European regulation emphasizes agent autonomy, safeguarding both the commercially sensitive data of market participants, cf. EU Parliament and EU Council (2019), and the critical infrastructure information of network operators, cf. EU Parliament and EU Council (2022). Electricity market processes in Europe account for inter-zonal congestions[1]. At the same time, intra-zonal issues are managed sequentially, cf. Weber et al. (2022), with Austria, Switzerland, and Germany employing cost-based redispatch systems, and the Nordic market, the Netherlands, and the United Kingdom utilizing counter-trading methods, cf. Grimm et al. (2022). To enhance intra-zonal congestion management and minimize its occurrence, German regulators, for instance, initiated reforms to bolster coordination among network operators, thereby augmenting redispatching capabilities, cf. Krueger et al. (2023), and implemented dynamic network tariffs to incentivize market participants to proactively prevent congestions, cf. Stute and Kühnbach (2023). Furthermore, debates around alternative solutions have emerged, e.g., proposing market-based redispatch systems, cf. Grimm et al. (2022) or local flexibility markets, cf. Radecke et al. (2019). However, despite the substantial increase in complexity of those frameworks, concerns persist about a lack of transparency and inefficiencies, cf. Grimm et al. (2022), as well as misplaced incentives, inducing, e.g., inc-dec-gaming, cf. Hirth et al. (2019).

On the other hand, the market design implemented in the US aims for a more integrated operation of markets and networks, based on a nodal pricing regime. These frameworks come at the expense of requiring market participants to disclose commercially sensitive information and delegate operational dispatch decisions to system operators, cf. Litvinov et al. (2019). To guarantee transparency for and non-discrimination of market participants, real-world implementations often involve the establishment of independent system operators (ISOs) or regional transmission organizations (RTOs), responsible for reliable system operation, market administration, and system planning, cf. Litvinov et al. (2019). However, while this unbundling is reasonable on a regulatory level to avoid distorted incentives regarding the

[1] E.g., on the level of countries via a flow-based market coupling, cf. Felten et al. (2021).

integrated operation of markets and networks, it is noteworthy that the disclosure of information and delegation of dispatch decisions is not an inherent feature of nodal pricing, cf. Hogan (1998). A key challenge to this design is the inherent complexity of the corresponding cyber-physical systems and the computational tractability of the resulting problems, cf. Litvinov et al. (2019). For instance, recent discussions focussing on a multi-period pricing regime aim to mitigate uncertainties posed by increasing renewable, cf. Hogan (2021). Furthermore, the extension of nodal prices to distribution networks is considered, especially with the growing presence of small-scale renewables and the potential of demand-side participation via so-called prosumers, cf. Hogan (2022). In addition, there is a growing emphasis on multi-energy coordination, as an improved cross-sectoral interaction is expected to unlock additional economic benefits, cf. Dall'Anese et al. (2017) and Pinson (2023). Meanwhile, challenges in the inter-regional coordination between multiple system operators, dubbed seams issues, persist, cf. Kavulla (2019).

1.2. Contributions and organization of the paper

Given the existing coordination frameworks and their implementational challenges, approaches that address confidentiality requirements and enable distributed market clearing seem promising. They may align with European regulation, enforcing the limited disclosure of information by market participants and network operators, while introducing the advantages of simultaneous operation of markets and networks. At the same time, such simultaneous frameworks have to offer solutions to the issues coming along with US systems, such as computational tractability, cross-sectoral coordination, and seams issues. This drives the methodical contributions of this paper, introducing a novel distributed framework with autonomous agents, facilitating the cross-sectoral coordination of highly interconnected multi-operator energy systems:

1. The framework is technology-agnostic, making it adaptable to various applications in multi-energy systems and enhancing its interpretability, particularly concerning economic transparency and financial settlement processes.
2. The approach effectively limits information exchange to bilateral communication between physically connected agents (network operators or market participants) via pairwise dependencies, ensuring agent autonomy and protecting the confidentiality of sensitive commercial and infrastructure information.

3. Furthermore, the framework supports a fully distributed and parallel co-optimization of all agents, removing the need for centralized coordination and effectively reducing communication steps per iteration.

In addition, the scalability and tractability of the proposed framework are assessed using a multi-energy system model. Based on different convex approximations and relaxations, the model takes inter-temporal and cross-sectoral constraints of a multitude of individual units into account. The proposed framework is furthermore applied to a comprehensive case study of Germany in a decarbonized scenario, focusing on the cross-sectoral operation of the electricity and district heating sector. In this context, the convergence is analyzed from a technical and economic perspective while introducing and assessing a series of potential indicators and metrics.

The paper is organized as follows: In Section 2, an overview of conceptual frameworks for simultaneous coordination is given, together with a thorough review of decomposition approaches. Subsequently, in Section 3, the novel distributed multi-operator coordination framework is introduced. Therefore, the general problem structure is introduced first before describing the structure of the distributed coordination framework. Thereupon, the application of the framework is explored in Section 4 by introducing a case study of Germany in a decarbonized scenario before assessing the results. The key findings are summarized in Section 5. In the Appendix supplemental material on the reformulation and decomposition of the general problem, coupling constraints, transfer payments between networks, primal and dual residuals, the cross-sectoral multi-energy system model and indicators for convergence, cf. Appendix A to E.

2. Conceptual frameworks for simultaneous coordination

The previously discussed challenges of simultaneous coordination frameworks have led to the exploration of various conceptual frameworks that aim to refine the coordination of electricity markets and network operations. These frameworks are instrumental in addressing the complex challenges associated with modern energy systems. In this context, centralized, hierarchical, and distributed types of simultaneous coordination frameworks can be distinguished, cf. Molzahn et al. (2017). In the following, the key elements of these conceptual frameworks are discussed and their applicability in the European context is assessed.

2.1. Centralized coordination

Centralized coordination—the archetype of today's ISOs and RTOs in the US—can be characterized by the presence of a single entity that handles market and network-related computations and dispatch decisions, cf. Molzahn et al. (2017). Considering cross-sectoral coordination, e.g., for natural gas and electricity systems, cf. He et al. (2018a), research often presumes the continuity of individual coordinators per sector, cf., e.g.,Chen et al. (2021). These approaches involve units being dispatched and operated by a single third party, often presumed to be the system operator (e.g., an ISO) of one of the sectors. While these frameworks simplify operational mechanisms and coordination efforts by limiting information exchange on the level of system operators, they come along with the requirement for disclosing sensitive economic information. Considering the European landscape, this centralized approach conflicts with the agent autonomy and confidentiality requirements, cf. EU Parliament and EU Council (2019) and EU Parliament and EU Council (2022). Centralized approaches are hardly implementable in Europe, especially when considering the multitude of highly interconnected network operators on transmission and distribution levels.

2.2. Hierarchical coordination

In contrast, hierarchical coordination approaches entail a tiered system of entities that perform market and network-related computations and dispatch decisions, culminating in a connection to a central controller, supervising the processes, cf. Molzahn et al. (2017). In this context, the concept of energy hubs gained recognition by laying the foundation for a coordinated operation of a multi-energy system, cf., e.g., Ding et al. (2022), utilizing a hierarchical coordination approach. However, there is a heterogeneity in research on the coordination between multiple systems. Proposals range from embedding energy hubs in already existing market structures, cf. Chen et al. (2018), to complex transactive market-clearing mechanisms, e.g., based on peer-to-peer trading, cf. Sorin et al. (2018) and Javadi et al. (2022). However, these approaches raise substantial concerns on a conceptual level, regarding complexity and the lack of transparency and scalability. As some approaches inherently require disclosing sensitive economic information, regulatory concerns in the European context arise.

2.3. Distributed coordination

Distributed coordination approaches are capable of operating without a centralized controller, i.e., with agents communicating directly with neighboring agents, cf. Molzahn et al. (2017). Existing conceptual frameworks

often either presume these agents to be network operators, cf., e.g., He et al. (2018b) and Wu et al. (2020), or market participants, cf., e.g., Sorin et al. (2018), exclusively. In the first case, it is often presumed that multi-energy areas are being operated by one single entity or by one third-party entity per sector, requiring the disclosure of sensitive economic information of market participants. In the second case, network-related constraints are neglected, or solutions lack scalability due to disproportionate computational efforts when applied to real-world applications, cf. Khorasany et al. (2018). Most of the existing conceptual frameworks for distributed coordination focus exclusively on engineering aspects and technical solutions, neglecting economic implications and interpretability. Recent research, cf. Schinke-Nendza et al. (2024a), addressed these issues by enabling cross-sectoral coordination, combining market-clearing and network operation with fully autonomous agents, i.e., market participants and network operators, and preserving the confidentiality of proprietary information of those agents. This approach integrates network subproblems, overcomes scalability issues of other distributed approaches, and aligns with the strict European confidentiality requirements for market participants, cf. Schinke-Nendza et al. (2024a). Yet, an extension of this distributed approach to a landscape of multiple network operators in the same sector, e.g., distinguished by transmission and distribution levels or different regions is so far missing. Such an approach should effectively tackle the seams issues between different network operators, cf. Litvinov et al. (2019). In this context, the disentanglement and decomposition of network-related constraints and cross-sectoral inter-temporal constraints of units deserve detailed investigation.

2.4. Decomposition approaches for distributed coordination

To achieve distributed coordination, decomposition methods are widely used, cf. Khorasany et al. (2018). By breaking down a complex, large-scale optimization problem into several subproblems, each can be solved independently and iteratively, cf. Ryu and Yin (2022). In this context, the alternating direction method of multipliers (ADMM) stands out as a versatile option, offering robust convergence and minimal structural requirements for subproblems, cf. Schinke-Nendza et al. (2024a). However, standard ADMM requires the sequential computation of two subproblems and forwarding of the primal solutions between them, cf. Ryu and Yin (2022). A direct extension to the case of multiple blocks of variables is not possible, cf. Chen et al. (2016). In contrast, an extension of ADMM to problems with a multi-block structure requires additional assumptions or modifications to guarantee convergence, cf. Ryu and Yin (2022). For instance,

Schinke-Nendza et al. (2024a) use the properties of the underlying problem, i.e., the separability of the objective functions and feasibility sets, to extend ADMM, without additional assumptions or modifications, to a multi-block case. However, these methods commonly necessitate a central coordination step, implying the need for a central coordinator, cf., e.g., Molzahn et al. (2017) and Mühlpfordt et al. (2021), and two communication steps per iteration, to forward primal and dual variable updates, cf. Wang et al. (2016).

In this context, Yang et al. (2022) provide a thorough discussion of ADMM variants suitable for problems with a multi-block structure and separable objectives that allow for a parallelizable implementation to solve the subproblems in a non-sequential distributed manner. For instance, the accelerated distributed augmented method (ADAL) allows for parallel multi-block structures by combining the Jacobian decomposition with a correction mechanism, cf. Chatzipanagiotis et al. (2015). This algorithm originates from the Diagonal Quadratic Approximation (DQA) and has been extended to address nonconvex problems, offering assurances of local convergence, cf. Yang et al. (2022). In addition, Deng et al. (2014) derive an algorithm by using Jacobian decomposition and adding proximal terms to the subproblem objectives. Due to its similarity to ADMM, the approach is dubbed proximal Jacobian ADMM (PJ-ADMM). Wang et al. (2014) find a more general form, the so-called parallel direction method of multipliers (PDMM), and can show that specific choices of the algorithm's parameters lead to PJ-ADMM.

Despite the advantages of parallel ADMM variants, their convergence rate remains unresolved, as highlighted by Ryu and Yin (2022). This issue is particularly pronounced in highly interconnected subproblems, as confirmed by the author's findings—not further elaborated hereinafter. Therefore, the method of Wang et al. (2016) is subsequently extended to establish a fully distributed and parallel process, eliminating the need for centralized coordination while limiting the exchange of information and effectively reducing the number of communication steps in each iteration. By integrating this improved approach with the reformulation of Schinke-Nendza et al. (2024a), a distributed framework is developed that facilitates the parallel optimization of autonomous agents with minimal coordination effort.

3. A distributed multi-operator coordination framework

In the following, first, the general problem structure is described, cf. Section 3.1. In the next step, the general architecture of the multi-operator coordination framework is introduced, followed by the reformulation and

decomposition of the general problem, cf. Section 3.2. A detailed elaboration of the equivalence of the general problem and the decomposed problem, based on a reformulation with pairwise coupling constraints and the introduction of a coordination step, can be found in Appendix A. Finally, in Section 3.3, the mathematical notation of the distributed multi-operator coordination framework is presented.

3.1. General problem structure

Regarding the cross-sectoral flexibility coordination in energy systems with multiple network operators, the general problem structure is depicted in Figure 1. In this context, a nodal pricing regime for the short-term operation of coupled energy systems is introduced to unify the market-clearing and network operations, following Schinke-Nendza et al. (2024a).[2]

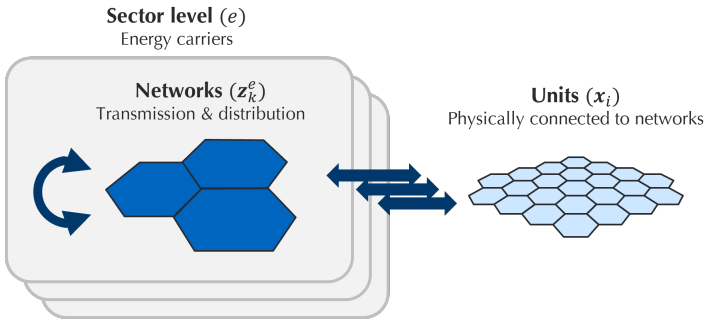

Figure 1: Considered problem structure with multiple networks (transmission and distribution) per energy sector and multiple (possibly cross-sectoral) units.

In general, three levels can be distinguished: The *sector* level, the level of *networks*, and the level of *units*. The sector level defines the energy carrier (index: e). Each sector encompasses one or more networks. Each network can be directly connected to any other network that transports the same energy carrier, e.g., linking transmission and distribution networks. Units can be connected to one or several networks, whereby they are connected only to one network per energy carrier. Hence, units can establish cross-sectoral connections, linking networks of different sectors indirectly. The

[2]Note that the introduction of a nodal pricing regime does not inherently come along with the properties of US American electricity markets, i.e., governance structures that lead to single-entity ISOs or RTOs with seams issues, or the requirement to disclose economically sensitive information.

corresponding energy carriers of these networks thereby serve as inputs or outputs of these units.

Presuming an omniscient single operator that operates across all energy carriers, the problem[3] of operating all units and networks can be written as

$$\min_{\boldsymbol{x},\boldsymbol{z}} \quad \sum_{i\in\mathcal{I}} f_i\left(\boldsymbol{x}_i\right) + \sum_{e\in\mathcal{E}}\sum_{k\in\mathcal{K}^e} g_k\left(\boldsymbol{z}_k\right) \tag{1a}$$

$$\text{s.t.} \quad \boldsymbol{A}_k^U\widetilde{\boldsymbol{x}}_k + \boldsymbol{A}_k^N\widetilde{\boldsymbol{z}}_{\neq k} + \boldsymbol{B}_k^N\widetilde{\boldsymbol{z}}_k = \boldsymbol{C}_k^N \quad : \boldsymbol{\lambda}_k, \quad \forall k \in \mathcal{K}^e, e \in \mathcal{E}, \tag{1b}$$

$$\boldsymbol{z}_k \in \mathcal{Z}_k, \qquad \forall k \in \mathcal{K}^e, e \in \mathcal{E}, \tag{1c}$$

$$\boldsymbol{x}_i \in \mathcal{X}_i, \qquad \forall i \in \mathcal{I}, \tag{1d}$$

where $\boldsymbol{x}_i$ are variables of units and $\boldsymbol{z}_k$ are variables of network k in sector e, with tilted symbols indicating coupling variables. In this context, the following aggregated notation of matrix-variable combinations is used

$$\boldsymbol{A}_k^U\widetilde{\boldsymbol{x}}_k = \sum_{i\in\mathcal{I}} \boldsymbol{A}_{i,k}^U\widetilde{\boldsymbol{x}}_{i,k}, \qquad \forall k \in \mathcal{K}^e, e \in \mathcal{E}, \tag{2a}$$

$$\boldsymbol{A}_k^N\widetilde{\boldsymbol{z}}_{\neq k} = \sum_{n\in\mathcal{K}\setminus\{k\}} \boldsymbol{A}_{n,k}^N\widetilde{\boldsymbol{z}}_{n,k}, \qquad \forall k \in \mathcal{K}^e, e \in \mathcal{E}, \tag{2b}$$

where $\widetilde{\boldsymbol{x}}_k$ denotes the vector that includes all unit coupling variables $\widetilde{\boldsymbol{x}}_{i,k}$ for connections to network k and $\widetilde{\boldsymbol{z}}_{\neq k}$ denotes the vector that includes all network coupling variables $\widetilde{\boldsymbol{z}}_{n,k} \subseteq \widetilde{\boldsymbol{z}}_n$ from other networks $n \in \mathcal{K}^e \setminus \{k\}$ to network k.[4] Therefore, $\widetilde{\boldsymbol{x}}_{i,k}$ is the vector of coupling variables of unit $i \in \mathcal{I}$ for network $k \in \mathcal{K}^e$ in sector $e \in \mathcal{E}$, which is a subvector of $\boldsymbol{x}_i$, the vector of all decision variables for unit i. We denote this as $\widetilde{\boldsymbol{x}}_{i,k} \subseteq \boldsymbol{x}_i$. Similarly, $\widetilde{\boldsymbol{z}}_k$ is defined for network $k \in \mathcal{K}^e$ as the vector of coupling variables to other

[3] For sake of simplicity, three notational conventions are introduced: First, despite considering a multi-period planning horizon, the time-step indices are dropped and all variables are implicitly defined to be time-variant. Second, matrices and vectors are expressed using bold letters and symbols. Third, the standard notation for sets to vectors is expanded. Particularly, the notation $\boldsymbol{a} \subseteq \boldsymbol{b}$ is used to express that $\boldsymbol{a}$ is a subvector of $\boldsymbol{b}$. In some cases $\boldsymbol{a} = \boldsymbol{b}$ might hold.

[4] If a certain unit $i \in \mathcal{I}$ is not connected to a network $k \in \mathcal{K}$, then $\boldsymbol{A}_i^U$ becomes zero, hence can be neglected. The same holds for interconnections to other networks and $\boldsymbol{A}_{n,k}^N$. For the sake of simplicity, the general case of full interconnection between all units and all networks is considered in the following. It is noteworthy that while alternative formulations can be found, such attempts would complicate subsequent derivations and obscure key relationships between dual and primal variables.

networks, with $\widetilde{\boldsymbol{z}}_k \subseteq \boldsymbol{z}_k$. Furthermore, the coupling variables of all networks excluding network k are aggregated as $\widetilde{\boldsymbol{z}}_{\neq k}$.

We presume that the *objective functions* of units and networks, defined by Eq. (1a), are convex and allow for block splitting, i.e., assuming that the objective functions of different units and networks are independent and separable. Then, objective functions can be written separately for units and networks for all energy carriers. Here, $f_i(\boldsymbol{x}_i)$ is the objective function of unit $i \in \mathcal{I}$, while $g_k(\boldsymbol{z}_k)$ is the objective function of network $k \in \mathcal{K}^e$ for energy carrier e. In general, the physical interconnection of networks and units can be reduced to nodal *balancing constraints* on the level of networks, cf. constraint (1b). These equations include all coupling variables that link multiple electricity networks, notably active power transmission and network state variables, like voltage angles. Therefore, the corresponding duals $\boldsymbol{\lambda}_k^e$ represent the locational marginal prices (LMPs). We elaborate on the coupling variables for electricity systems in Appendix B. Considering the feasibility sets of units and networks, i.e., $\mathcal{X}_i$ and $\mathcal{Z}_k$, convexity and separability are assumed in this paper. Hence, the convex feasibility sets of each entity, either unit or network, are independent of each other, cf. Eq. (1c)-(1d). When considering a specific entity, there might be inter-temporal relations between variables, e.g., filling levels. However, these do not introduce a coupling between entities, as interconnections are exclusively given by Eq. (1b).

3.2. Reformulated problem and decomposition

The intended architecture of the distributed coordination framework, motivating the subsequent reformulation and decomposition, is depicted in Fig. 2. It consists of *four phases* per iteration that are decoupled and independent for each agent: the optimization phase, the communication phase, the coordination step, and the price updates.[5] A detailed description of the assigned variables follows hereinafter, see problem (3). For all agents, each iteration starts with the *optimization phase*, where all agents, i.e., networks and units, optimize themselves in parallel based on the retrieved primal and dual variables of the previous iteration. Thereupon, in the *communication phase*, the new results, i.e., $\boldsymbol{z}_k$, $\boldsymbol{\zeta}_k$ and $\boldsymbol{x}_i$, are forwarded to all directly connected agents. Subsequently, in the *coordination step*, each agent updates the primal coordination variables, i.e., $\left\{\boldsymbol{\psi}_{k,n}^{N,src}, \boldsymbol{\psi}_{k,n}^{N,dest}\right\} \subseteq \boldsymbol{\psi}_k^N$ and $\boldsymbol{\psi}_{k,i}^{U,dest} \subseteq \boldsymbol{\psi}_k^{U,dest}$ for all networks k, and $\boldsymbol{\psi}_{i,k}^{U,src} \subseteq \boldsymbol{\psi}_i^{U,src}$ for all units i. These

[5] Note that between two iterations, no communication between agents is required.

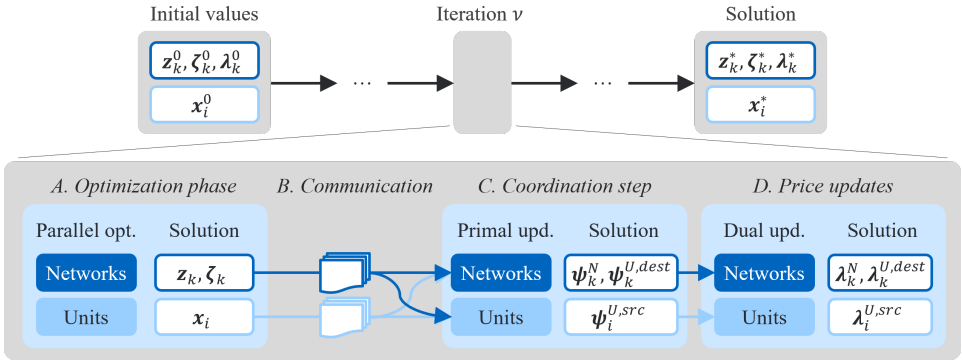

Figure 2: Iterative architecture of the distributed coordination framework and parallel information processing of networks and units in each iteration.

updates are based on the results $\boldsymbol{z}_k$, $\boldsymbol{\zeta}_k$ and $\boldsymbol{x}_i$ obtained from interconnected agents, i.e., either units or networks, during the preceeding communication step. In the *price update phase*, each agent updates its dual variables, i.e., the prices $\boldsymbol{\lambda}_{k,n}^{N,src}$, $\boldsymbol{\lambda}_{k,n}^{N,dest}$, $\boldsymbol{\lambda}_{k,i}^{U,src}$, and $\boldsymbol{\lambda}_{k,i}^{U,dest}$, for all interconnections with other agents. These updates use only the own results of the last optimization phase and the updated primal variables retrieved from the coordination step. Note that all phases are completely decoupled, i.e., all agents can update primal and dual variables and optimize themselves entirely independently and in parallel. Communication takes place in the communication phase exclusively in the form of operative results, thus preserving the subproblems' confidentiality. This process is repeated iteratively until convergence can be observed and a final solution is found.

The previously introduced single operator problem (1) can be reformulated without loss of generality, based on the introduction of *pairwise coupling constraints* and a *coordination step* as

$$\min_{\boldsymbol{x},\boldsymbol{z}} \quad \sum_{i\in\mathcal{I}} f_i\left(\boldsymbol{x}_i\right) + \sum_{e\in\mathcal{E}}\sum_{k\in\mathcal{K}^e} g_k\left(\boldsymbol{z}_k\right) \tag{3a}$$

$$\text{s.t.} \quad \widetilde{\boldsymbol{z}}_{n,k} = \boldsymbol{\psi}_{n,k}^{N,src} \quad : \boldsymbol{\lambda}_{k,n}^{N,src}, \quad \forall n \in \mathcal{K}^e \setminus \{k\}, k \in \mathcal{K}^e, e \in \mathcal{E}, \tag{3b}$$

$$\boldsymbol{\zeta}_{k,n}^{N} = \boldsymbol{\psi}_{k,n}^{N,dest} \quad : \boldsymbol{\lambda}_{k,n}^{N,dest}, \quad \forall n \in \mathcal{K}^e \setminus \{k\}, k \in \mathcal{K}^e, e \in \mathcal{E}, \tag{3c}$$

$$\boldsymbol{\psi}_{n,k}^{N,src} = \boldsymbol{\psi}_{k,n}^{N,dest} \quad : \boldsymbol{\lambda}_{k,n}^{N}, \quad \forall n \in \mathcal{K}^e \setminus \{k\}, k \in \mathcal{K}^e, e \in \mathcal{E}, \tag{3d}$$

$$\widetilde{\boldsymbol{x}}_{i,k} = \boldsymbol{\psi}_{i,k}^{U,src}, \quad : \boldsymbol{\lambda}_{k,i}^{U,src}, \quad \forall i \in \mathcal{I}, k \in \mathcal{K}^e, e \in \mathcal{E}, \tag{3e}$$

$$\boldsymbol{\zeta}_{k,i}^{U} = \boldsymbol{\psi}_{k,i}^{U,dest}, \quad : \boldsymbol{\lambda}_{k,i}^{U,dest}, \quad \forall i \in \mathcal{I}, k \in \mathcal{K}^e, e \in \mathcal{E}, \tag{3f}$$

$$\boldsymbol{\psi}_{i,k}^{U,src} = \boldsymbol{\psi}_{k,i}^{U,dest}, \qquad : \boldsymbol{\lambda}_{k,i}^{U}, \qquad \forall i \in \mathcal{I}, k \in \mathcal{K}^e, e \in \mathcal{E}, \tag{3g}$$

$$\boldsymbol{z}_k, \boldsymbol{\zeta}_k \in \mathcal{Z}_k^{\zeta}, \qquad \forall k \in \mathcal{K}^e, e \in \mathcal{E}, \tag{3h}$$

$$\boldsymbol{x}_i \in \mathcal{X}_i, \qquad \forall i \in \mathcal{I}. \tag{3i}$$

with $\{\widetilde{\boldsymbol{x}}_{i,k}, \boldsymbol{x}_i\} \subseteq \boldsymbol{x}$ the unit-related variables, $\{\boldsymbol{z}_k, \widetilde{\boldsymbol{z}}_{n,k}, \boldsymbol{\zeta}_k\} \subseteq \boldsymbol{z}$ the network-related variables, and $\left\{\boldsymbol{\psi}_{n,k}^{N,src}, \boldsymbol{\psi}_{k,n}^{N,dest}, \boldsymbol{\psi}_{i,k}^{U,src}, \boldsymbol{\psi}_{k,i}^{U,dest}\right\} \subseteq \boldsymbol{\psi}_k$ the variables assigned to the coordination step.[6] A comprehensive derivation of the equivalence of the general problem (1) and the decomposed problem (3) can be found in Appendix A. Here, the auxiliary variables $\{\boldsymbol{\zeta}_{k,n}^{N}, \boldsymbol{\zeta}_{k,i}^{U}\} \subseteq \boldsymbol{\zeta}_k$ follow from the introduction of *bilateral coupling constraints* (while assigning the balancing constraints to the feasibility sets of the corresponding networks), while auxiliary variables $\boldsymbol{\psi}_k$ follow from the *coordination step*. Here, index *src* references the source (i.e., a network or unit), and index *dest* references the destination network connected through the balancing constraint. The coupling in problem (3) now consists of bilateral equality constraints exclusively, which allows for the following decomposition.

As a next step, ADMM is applied to problem (3). This yields independently solvable subproblems for units, networks, and the coordination step in each iteration ν. The aggregated subproblem for all networks is

$$\begin{aligned} \min_{\boldsymbol{z}} \quad & \sum_{e \in \mathcal{E}} \sum_{k \in \mathcal{K}^e} \Bigg[g_k\left(\boldsymbol{z}_k\right) + \sum_{n \in \mathcal{K}^e \setminus \{k\}} \xi_\rho \left[\widetilde{\boldsymbol{z}}_{k,n}, \left(\boldsymbol{\psi}_{k,n}^{N,src}\right)^\nu, \left(\boldsymbol{\lambda}_{k,n}^{N,src}\right)^\nu \right] \\ & + \sum_{n \in \mathcal{K}^e \setminus \{k\}} \xi_\rho \left[\boldsymbol{\zeta}_{k,n}^{N}, \left(\boldsymbol{\psi}_{k,n}^{N,dest}\right)^\nu, \left(\boldsymbol{\lambda}_{k,n}^{N,dest}\right)^\nu \right] \\ & + \sum_{i \in \mathcal{I}} \xi_\rho \left[\boldsymbol{\zeta}_{k,i}^{U}, \left(\boldsymbol{\psi}_{k,i}^{U,dest}\right)^\nu, \left(\boldsymbol{\lambda}_{k,i}^{U,dest}\right)^\nu \right] \Bigg] \end{aligned} \tag{4a}$$

$$\text{s.t.} \quad \boldsymbol{z}_k, \boldsymbol{\zeta}_k \in \mathcal{Z}_k^{\zeta}, \qquad \forall k \in \mathcal{K}^e, e \in \mathcal{E}, \tag{4b}$$

with the result of problem (4) being denoted as $(\boldsymbol{z})^{\nu+1}$, where $\xi_\rho\left[\cdot\right]$ is the regularization term of ADMM that is defined as

$$\xi_\rho \left[\boldsymbol{\alpha}, (\boldsymbol{\beta})^\nu, (\boldsymbol{\lambda})^\nu \right] = \left\langle (\boldsymbol{\lambda})^\nu, \boldsymbol{\alpha} \right\rangle + \frac{\rho}{2} \left\| \boldsymbol{\alpha} - (\boldsymbol{\beta})^\nu \right\|_2^2, \tag{5}$$

[6] Note that the variables' subscript indices (e.g. indices k, n) denote their assignment and interconnection: the first index indicates the entity to whose subproblem the variable is assigned assigned (e.g. index k), and the second index specifies the subproblem of the interconnected entity (e.g. index n).

with ρ the ADMM-related penalty parameter.[7] Note that the objective function and the constraints of this aggregated problem are separable by networks, which will be elaborated further in Section 3.3.1. Similarly, the subproblem containing all units follows as

$$\min_{\boldsymbol{x}} \quad \sum_{i\in\mathcal{I}}\left[f_i\left(\boldsymbol{x}_i\right)+\sum_{e\in\mathcal{E}}\sum_{k\in\mathcal{K}^e}\xi_\rho\left[\widetilde{\boldsymbol{x}}_{i,k},\left(\boldsymbol{\psi}_{i,k}^{U,src}\right)^{\nu},\left(\boldsymbol{\lambda}_{k,i}^{U,src}\right)^{\nu}\right]\right] \tag{6a}$$

$$\text{s.t.} \quad \boldsymbol{x}_i\in\mathcal{X}_i, \qquad \forall i\in\mathcal{I}, \tag{6b}$$

with the result of problem (6) being denoted as $(\boldsymbol{x})^{\nu+1}$. The results of problems (4) and (6) are then handed over to the subproblem of the coordination step that is defined as

$$\begin{aligned}\min_{\boldsymbol{\psi}_k} \quad & \sum_{e\in\mathcal{E}}\sum_{k\in\mathcal{K}^e}\Bigg[\sum_{n\in\mathcal{K}^e\setminus\{k\}}\xi_\rho\left[\boldsymbol{\psi}_{n,k}^{N,src},\left(\widetilde{\boldsymbol{z}}_{n,k}\right)^{\nu+1},-\left(\boldsymbol{\lambda}_{k,n}^{N,src}\right)^{\nu}\right]\\ &+\sum_{n\in\mathcal{K}^e\setminus\{k\}}\xi_\rho\left[\boldsymbol{\psi}_{k,n}^{N,dest},\left(\boldsymbol{\zeta}_{k,n}^{N}\right)^{\nu+1},-\left(\boldsymbol{\lambda}_{k,n}^{N,dest}\right)^{\nu}\right]\\ &+\sum_{i\in\mathcal{I}}\xi_\rho\left[\boldsymbol{\psi}_{i,k}^{U,src},\left(\widetilde{\boldsymbol{x}}_{i,k}^{e}\right)^{\nu+1},-\left(\boldsymbol{\lambda}_{k,i}^{U,src}\right)^{\nu}\right]\\ &+\sum_{i\in\mathcal{I}}\xi_\rho\left[\boldsymbol{\psi}_{k,i}^{U,dest},\left(\boldsymbol{\zeta}_{k,i}^{U}\right)^{\nu+1},-\left(\boldsymbol{\lambda}_{k,i}^{U,dest}\right)^{\nu}\right]\Bigg]\end{aligned} \tag{7a}$$

$$\text{s.t.} \quad \boldsymbol{\psi}_{n,k}^{N,src}=\boldsymbol{\psi}_{k,n}^{N,dest} \quad :\boldsymbol{\lambda}_{k,n}^{N}, \quad \forall n\in\mathcal{K}^e\setminus\{k\}, k\in\mathcal{K}^e, e\in\mathcal{E}, \tag{7b}$$

$$\boldsymbol{\psi}_{i,k}^{U,src}=\boldsymbol{\psi}_{k,i}^{U,dest}, \quad :\boldsymbol{\lambda}_{k,i}^{U}, \quad \forall i\in\mathcal{I}, k\in\mathcal{K}^e, e\in\mathcal{E}, \tag{7c}$$

with the result of problem (7) being denoted as $(\boldsymbol{\psi}_k^e)^{\nu+1}$.

Using the results of subproblems (4) to (7), the dual variable updates can be computed independently for networks $n,k\in\mathcal{K}^e, e\in\mathcal{E}$, with $n\neq k$, as

$$\left(\boldsymbol{\lambda}_{k,n}^{N,src}\right)^{\nu+1}=\left(\boldsymbol{\lambda}_{k,n}^{N,src}\right)^{\nu}+\varphi\rho\left[\left(\widetilde{\boldsymbol{z}}_{n,k}^{e}\right)^{\nu+1}-\left(\boldsymbol{\psi}_{n,k}^{N,src}\right)^{\nu+1}\right], \tag{8a}$$

$$\left(\boldsymbol{\lambda}_{k,n}^{N,dest}\right)^{\nu+1}=\left(\boldsymbol{\lambda}_{k,n}^{N,dest}\right)^{\nu}+\varphi\rho\left[\left(\boldsymbol{\zeta}_{k,n}^{N}\right)^{\nu+1}-\left(\boldsymbol{\psi}_{k,n}^{N,dest}\right)^{\nu+1}\right]. \tag{8b}$$

[7] For sake of simplicity any constant terms are dropped. Note that $\langle x,y\rangle = x^\top y = \sum_i x_i y_i$ describes the standard inner product.

For interconnections between unit $i \in \mathcal{I}$ and network $k \in \mathcal{K}^e$ in sector $e \in \mathcal{E}$, the dual variable updates follow as

$$\left(\boldsymbol{\lambda}_{k,i}^{U,src}\right)^{\nu+1} = \left(\boldsymbol{\lambda}_{k,i}^{U,src}\right)^{\nu} + \varphi\rho\Big[\left(\widetilde{\boldsymbol{x}}_{i,k}^{e}\right)^{\nu+1} - \left(\boldsymbol{\psi}_{i,k}^{U,src}\right)^{\nu+1}\Big], \tag{9a}$$

$$\left(\boldsymbol{\lambda}_{k,i}^{U,dest}\right)^{\nu+1} = \left(\boldsymbol{\lambda}_{k,i}^{U,dest}\right)^{\nu} + \varphi\rho\Big[\left(\boldsymbol{\zeta}_{k,i}^{U}\right)^{\nu+1} - \left(\boldsymbol{\psi}_{k,i}^{U,dest}\right)^{\nu+1}\Big]. \tag{9b}$$

Here, φ is the dual extrapolation parameter, cf. Ryu and Yin (2022).

3.3. Structure of the distributed coordination framework

The general architecture of the distributed coordination framework and the related phases are depicted in Fig. 2. In the following sections, the mathematical description and the individual subproblems of each phase are presented. For the optimization phase, this includes the individual network and unit subproblems. Thereupon, the intricacies of the coordination step and the dual variable updates are specified.

3.3.1. Network subproblems

Considering problem (4), the feasibility sets $\boldsymbol{z}_k, \boldsymbol{\zeta}_k \in \mathcal{Z}_k^{\zeta}$ and objective functions $g_k(\boldsymbol{z}_k)$ are separable for all networks $k \in \mathcal{K}^e$ and sectors $e \in \mathcal{E}$. The introduced auxiliary variables $\boldsymbol{\zeta}$ and $\boldsymbol{\psi}$ successfully decouple the network subproblems. All coupling constraints are relocated to the objective function by means of the regularization terms. However, as auxiliary variable $(\boldsymbol{\psi})^{\nu}$ and prices $(\boldsymbol{\lambda})^{\nu}$ are constant values of the previous iteration ν, the subproblem of all networks decomposes into $|\mathcal{K}^e|$ independent problems in sector e. Consequently, the problem of a single network $k \in \mathcal{K}^e$ can be written as

$$\begin{aligned}
\min_{\boldsymbol{z}_k} \quad & g_k(\boldsymbol{z}_k) + \sum_{n \in \mathcal{K}^e \setminus \{k\}} \left[\left\langle \left(\boldsymbol{\lambda}_{k,n}^{N,src}\right)^{\nu}, \widetilde{\boldsymbol{z}}_{k,n} \right\rangle + \frac{\rho}{2}\left\| \widetilde{\boldsymbol{z}}_{k,n} - \left(\boldsymbol{\psi}_{k,n}^{N,src}\right)^{\nu} \right\|_2^2\right] \\
& + \sum_{n \in \mathcal{K}^e \setminus \{k\}} \left[\left\langle \left(\boldsymbol{\lambda}_{k,n}^{N,dest}\right)^{\nu}, \boldsymbol{\zeta}_{k,n}^{N} \right\rangle + \frac{\rho}{2}\left\| \boldsymbol{\zeta}_{k,n}^{N} - \left(\boldsymbol{\psi}_{k,n}^{N,dest}\right)^{\nu} \right\|_2^2\right] \\
& + \sum_{i \in \mathcal{I}} \left[\left\langle \left(\boldsymbol{\lambda}_{k,i}^{U,dest}\right)^{\nu}, \boldsymbol{\zeta}_{k,i}^{U} \right\rangle + \frac{\rho}{2}\left\| \boldsymbol{\zeta}_{k,i}^{U} - \left(\boldsymbol{\psi}_{k,i}^{U,dest}\right)^{\nu} \right\|_2^2\right]
\end{aligned} \tag{10a}$$

$$\text{s.t.} \quad \boldsymbol{z}_k, \boldsymbol{\zeta}_k \in \mathcal{Z}_k^{\zeta}, \tag{10b}$$

with the result of problem (10) being denoted as $(\boldsymbol{z}_k)^{\nu+1}$. Similar to Schinke-Nendza et al. (2024a), the objective function in the network subproblem can

be subdivided into three types of components: First, the original objective function $g_k(\boldsymbol{z}_k)$, second, the inner products $\langle \cdot, \cdot \rangle$ of dual and primal variables representing either procurement costs or revenues[8], and third, the augmented Lagrangian terms $\| \cdot \|_2^2$ that aim at minimizing the difference between the agents' primal variables.

3.3.2. Unit subproblems

Considering problem (6), the feasibility sets $\mathcal{X}_i$ and objective functions $f_i(\boldsymbol{x}_i)$ are also separable for all $i \in \mathcal{I}$, i.e., subproblems of all units are not interrelated to one another. The same holds for the regularization term that establishes a connection to networks k in sectors e. Therefore, the subproblem of all units decomposes into $|\mathcal{I}|$ independent problems and the problem of a single unit $i \in \mathcal{I}$ can be written as

$$\min_{\boldsymbol{x}_i} \quad f_i(\boldsymbol{x}_i) + \sum_{e \in \mathcal{E}} \sum_{k \in \mathcal{K}^e} \left[\left\langle \left(\boldsymbol{\lambda}_{k,i}^{U,src} \right)^{\nu}, \widetilde{\boldsymbol{x}}_{i,k} \right\rangle + \frac{\rho}{2} \left\| \widetilde{\boldsymbol{x}}_{i,k} - \left(\boldsymbol{\psi}_{i,k}^{U,src} \right)^{\nu} \right\|_2^2 \right] \tag{11a}$$

$$\text{s.t.} \quad \boldsymbol{x}_i \in \mathcal{X}_i, \tag{11b}$$

with the result of problem (11) being denoted as $(\boldsymbol{x}_i)^{\nu+1}$. Similarly to the network subproblem, the objective function in the unit subproblem can also be subdivided into three types of components with respect to Eq. (5) and problem (11): First, the original objective function $f_i(\boldsymbol{x}_i)$, second, the inner products $\langle \cdot, \cdot \rangle$ of dual and primal variables representing either procurement costs for buying energy or revenues for selling energy, and third, the augmented Lagrangian terms $\| \cdot \|_2^2$ that aim at minimizing the difference between the unit's and network's primal variables.

3.3.3. Coordination step

Regarding the coordination step, i.e., problem (7), a close examination reveals two interesting properties: The objective function is composed of regularization terms exclusively that are all separable. Furthermore, the feasibility sets consist of bilateral equality constraint exclusively, hence linking either the variables of two networks or the variables of a network and a unit. Thereupon, the network-connecting subproblems, with variables $\boldsymbol{\psi}^N$, and the network-unit-related subproblem, with variables $\boldsymbol{\psi}^U$, can be separated. These subproblems can be solved independently for each connection.

[8] Considering interconnections with other networks, this term values the exchanged energy and corresponds to transfer payments between network operators, see Appendix C. For interconnections with units, the network has to procure or sell energy.

In addition, an analytical solution to both subproblems can be found, cf. Boyd et al. (2011). For the network-connecting subproblem, describing the interconnection of two networks $n, k \in \mathcal{K}^e$, with $n \neq k$, in sector $e \in \mathcal{E}$, the solution is

$$\left(\boldsymbol{\psi}_{n,k}^{N,src}\right)^{\nu+1} = \frac{(\widetilde{\boldsymbol{z}}_{n,k})^{\nu+1} + \left(\boldsymbol{\zeta}_{k,n}^{N}\right)^{\nu+1}}{2} + \frac{\left(\boldsymbol{\lambda}_{k,n}^{N,src}\right)^{\nu} + \left(\boldsymbol{\lambda}_{k,n}^{N,dest}\right)^{\nu}}{2\rho}, \quad (12)$$

with $\left(\boldsymbol{\psi}_{n,k}^{N,src}\right)^{\nu+1} = \left(\boldsymbol{\psi}_{k,n}^{N,dest}\right)^{\nu+1}$, which corresponds to the results of the coordination step (7) for network connections. For the subproblem establishing an connection between unit $i \in \mathcal{I}$ and network $k \in \mathcal{K}^e$ and sectors $e \in \mathcal{E}$, the solution follows as

$$\left(\boldsymbol{\psi}_{i,k}^{U,src}\right)^{\nu+1} = \frac{(\widetilde{\boldsymbol{x}}_{i,k})^{\nu+1} + \left(\boldsymbol{\zeta}_{k,i}^{U}\right)^{\nu+1}}{2} + \frac{\left(\boldsymbol{\lambda}_{k,i}^{U,src}\right)^{\nu} + \left(\boldsymbol{\lambda}_{k,i}^{U,dest}\right)^{\nu}}{2\rho}, \quad (13)$$

with $\left(\boldsymbol{\psi}_{i,k}^{U,src}\right)^{\nu+1} = \left(\boldsymbol{\psi}_{k,i}^{U,dest}\right)^{\nu+1}$, in line with the unit-related results of the coordination step (7). In this context, it is noteworthy that with the subsequent findings, presented in Eq. (16), imply that the averaging term of dual variables cancels out in Eq. (12) and (13).

3.3.4. Dual variable updates

The dual variable updates can be computed independently for the network-related and unit-related variables. Using the results of subproblems (10) to (13), the dual variable updates for two interconnected networks $n, k \in \mathcal{K}^e, e \in \mathcal{E}$, with $n \neq k$, follow to

$$\left(\boldsymbol{\lambda}_{k,n}^{N,src}\right)^{\nu+1} = \left(\boldsymbol{\lambda}_{k,n}^{N,src}\right)^{\nu} + \varphi^{\nu}\rho^{\nu}\left[(\widetilde{\boldsymbol{z}}_{n,k})^{\nu+1} - \left(\boldsymbol{\psi}_{n,k}^{N,src}\right)^{\nu+1}\right], \quad (14a)$$

$$\left(\boldsymbol{\lambda}_{k,n}^{N,dest}\right)^{\nu+1} = \left(\boldsymbol{\lambda}_{k,n}^{N,dest}\right)^{\nu} + \varphi^{\nu}\rho^{\nu}\left[(\boldsymbol{\zeta}_{k,n}^{N})^{\nu+1} - \left(\boldsymbol{\psi}_{k,n}^{N,dest}\right)^{\nu+1}\right]. \quad (14b)$$

For interconnections between unit $i \in \mathcal{I}$ and network $k \in \mathcal{K}^e$ in sector $e \in \mathcal{E}$, the dual variable updates follow as

$$\left(\boldsymbol{\lambda}_{k,i}^{U,src}\right)^{\nu+1} = \left(\boldsymbol{\lambda}_{k,i}^{U,src}\right)^{\nu} + \varphi^{\nu}\rho^{\nu}\left[(\widetilde{\boldsymbol{x}}_{i,k})^{\nu+1} - \left(\boldsymbol{\psi}_{i,k}^{U,src}\right)^{\nu+1}\right], \quad (15a)$$

$$\left(\boldsymbol{\lambda}_{k,i}^{U,dest}\right)^{\nu+1} = \left(\boldsymbol{\lambda}_{k,i}^{U,dest}\right)^{\nu} + \varphi^{\nu}\rho^{\nu}\left[(\boldsymbol{\zeta}_{k,i}^{U})^{\nu+1} - \left(\boldsymbol{\psi}_{k,i}^{U,dest}\right)^{\nu+1}\right]. \quad (15b)$$

Examining Eq. (12) and (13) in combination with Eq. (14) and (15) reveals that for the dual variables of iteration ν the following identities hold

$$\left(\boldsymbol{\lambda}_{k,n}^{N,src}\right)^{\nu} = -\left(\boldsymbol{\lambda}_{k,n}^{N,dest}\right)^{\nu}, \qquad \text{and} \qquad \left(\boldsymbol{\lambda}_{k,i}^{U,src}\right)^{\nu} = -\left(\boldsymbol{\lambda}_{k,i}^{U,dest}\right)^{\nu}, \tag{16}$$

if Eq. (16) holds for the initial values (i.e., $\nu = 0$), and ρ^{ν} and φ^{ν} are identical across Eqs. (14a) and (14b), and Eqs. (15a) and (15b) within each iteration.. Hence, in each iteration $\boldsymbol{\lambda}_{k,n}^{N,src}$ and $\boldsymbol{\lambda}_{k,n}^{N,dest}$ are identical and equal to $\boldsymbol{\lambda}_{k,n}^{N}$, while the same holds for $\boldsymbol{\lambda}_{k,n}^{U,src}$ and $\boldsymbol{\lambda}_{k,n}^{U,dest}$, with respect to $\boldsymbol{\lambda}_{k,n}^{U}$.

To improve convergence, parameters ρ^{ν} and φ^{ν} can be introduced that vary in each iteration, based on the primal and dual residuals, r^{ν} and s^{ν}.[9] To accelerate convergence, an algorithm with proven effectiveness is employed, cf., e.g., Schinke-Nendza et al. (2024a). Thereby, ρ^{ν} is modified based on Euclidean norms for primal and dual residuals

$$\rho^{\nu+1} := \begin{cases} \tau\rho^{\nu} & \text{if } \|r^{\nu}\|_2 > \mu \|s^{\nu}\|_2 , \\ \rho^{\nu}/\tau & \text{if } \|s^{\nu}\|_2 > \mu \|r^{\nu}\|_2 , \\ \rho^{\nu} & else, \end{cases} \tag{17}$$

with $\mu > 1$ and $\tau > 1$. When updating parameters ρ^{ν}, also the dual extrapolation parameter φ^{ν} needs to be adapted to ensure convergence. Here, Ryu and Yin (2022) derive convergence guarantees for $\rho > 0$ and $\varphi \in (0, 2)$, where $0 < \varphi < \frac{1+\sqrt{5}}{2}$ holds for large ρ and $\frac{1+\sqrt{5}}{2} \leq \varphi < 2$ for small ρ.

The dual variable updates, defined by Eq. (14) and (15), can be processed in a completely distributed manner by each agent. The same holds for the coordination step, i.e., upon receiving the results of any interconnected agent, the primal updates for $(\boldsymbol{\psi}_k)^{\nu+1}$ can be processed independently by each agent. Therefore, these two steps, together with the updates of ρ^{ν} and φ^{ν}, based on Eq. (17), can be assigned to each agent individually as an additional task before optimizing themselves.

To avoid issues due to communication errors, it might be a save option for agents to exchange all intermediate results with connected agents. Besides the results of the optimization, this might include the primal variables of the coordination step, dual variables together with parameters ρ^{ν} and φ^{ν}, to ensure alignment of interconnected agents. In case of a communication error, deviations might occur in the variables of the coordination step, the dual variables, or the parameters. In such a case, both agents could simply use

[9] The definitions of these norms of residuals are given in Appendix D.

the last matching results and re-join the iterative coordination procedure. The resulting process is then dubbed as asynchronous ADMM, cf. Zhang and Kwok (2014). As long as communication errors, i.e., the asynchrony, are not prevalent in the process, theoretical convergence guarantees remain in force, cf. Zhang and Kwok (2014)

However, when assigning market-related tasks to network operators, regulatory concerns regarding transparency, discrimination, and disincentives arise, cf. Hogan (1998). Here, a segregation of ownership rights and operational responsibilities, e.g., via an unbundling into network owners and independent system operators, can be effective, cf. Hogan (1998). Alternatively, the introduction of additional regulatory entities responsible for updating and communicating prices to agents could be a viable solution.

4. Application

In this section, a comprehensive case study is presented that applies the distributed coordination framework with autonomous agents, and the corresponding results are discussed, from a technical and economic perspective.

4.1. Case study

To analyze the properties and intricacies of the proposed distributed coordination framework, this paper focuses on the cross-sectoral and intertemporal coupling of subproblems of a multitude of autonomous agents in the electricity and heat sector in an hourly resolution. To this end, an excerpt of the data and technology models presented in Schinke-Nendza et al. (2024b) is used. A detailed description of the used unit and network-related models of the electricity and heat sector can be found in Appendix E.

Table 1: Number of units and maximum capacity (in GW) in electricity and heat sector per technology.

Technology	**No. Units**	**Max. capacity (in GW)**	
		Electricity	Heat
GFPP	205	98.05	-
CHP all	161	49.33	16.97
CHP (BP)	64	1.90	1.90
CHP (EC)	97	47.42	15.07
PtH	55	2.62	2.62
Heating Plants	17	-	9.73

Table 2: Number of aggregated units and supplied or consumed energy (in GWh) of technologies in the electricity and heat sector for the considered 6-hour period.

Technology	**No. Units**	**Energy (in GWh)**	
		Electricity	Heat
Wind & PV	2,181	105.38	-
Hydro ROR	42	15.10	-
El. Demand	2,835	412.34	-
Heat Demand	35	-	7.48
Const. Heat Demand	57	-	20.55

Table 3: Number of all and coupling elements in electric transmission and distribution networks.

Network		**Nodes**		**Branches**	
		All	Coupling	All	Coupling
Transm.	1	251	93	472	63
	2	220	121	552	145
	3	143	40	276	22
	4	98	26	226	15
Distrib.	1	998	8	1,213	8
	2	1,212	15	1,589	20
	3	826	2	939	3
	4	823	63	1,281	116
	5	841	4	1,014	4

The input data of this case study consists of the first 6 hours of an exemplary day[10] in a decarbonized scenario for Germany in the year 2050. It is based on the EL 95 scenario provided in Deutsche Energie-Agentur GmbH (2018), envisioning a comprehensive electrification of end-use energy sectors by 2050 while targeting a 95% reduction in CO_2 emissions.

In this scenario, thermal power plants use green methane as a fuel, while technical improvements enhance the power plants' flexibility. Therefore, the impact of ramp rates, together with minimal operation times and down-times, is assumed to be negligible for combined heat and power (CHP) and gas-fired power plants (GFPPs). Table 1 summarizes the number of units and maximum capacity (in GW) for electricity and heat. The generation of renewables, together with the electricity and heat demand (in GWh),

[10]For this purpose, a winter day (in calendar week 39) with high residual load, i.e., with low renewable infeed, is considered.

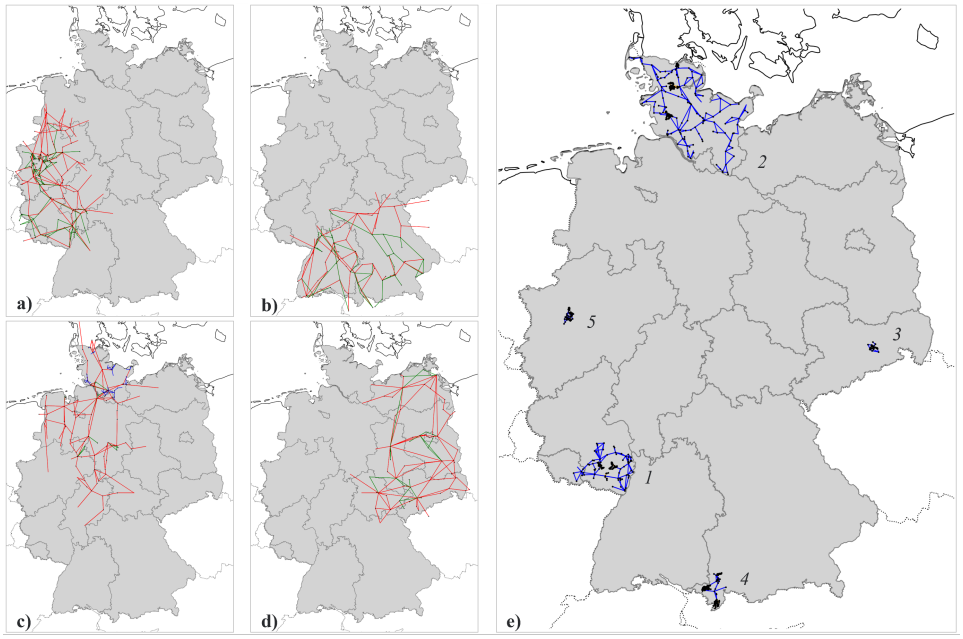

Figure 3: Electricity networks: a) - d) transmission networks 1 to 4 and e) distribution networks 1 to 5, with coloring acc. to voltage levels: 380 kV (red), 220 kV (green), 110 kV (blue), 20 kV (orange) and 0.4 kV (yellow).

are depicted in Tab. 2. Regarding the electricity infrastructure, four transmission and five distribution networks are considered as depicted in Fig. 3, with technical details given in Tab. 3. Regarding the heat sector, 74 district heating networks are incorporated, where the demand for (residential and commercial) space heating is denoted as 'heat demand', while the industrial heat demand is denoted as 'constant heat demand.'

4.2. Results

Subsequently, the results of applying the proposed distributed coordination framework to a large-scale application of the electricity and heat sector are presented, considering both a technical and an economic perspective. In this context, the technical perspective includes a detailed assessment of primal variables, indicating dispatch decisions and energy-related quantities. Meanwhile, from an economic perspective, dual variables and their product with corresponding primal variables, yielding revenues and costs, are of interest, especially for the financial settlement process.

In a first step, the convergence of the proposed distributed coordination framework is assessed. A major indicator for convergence of the distributed

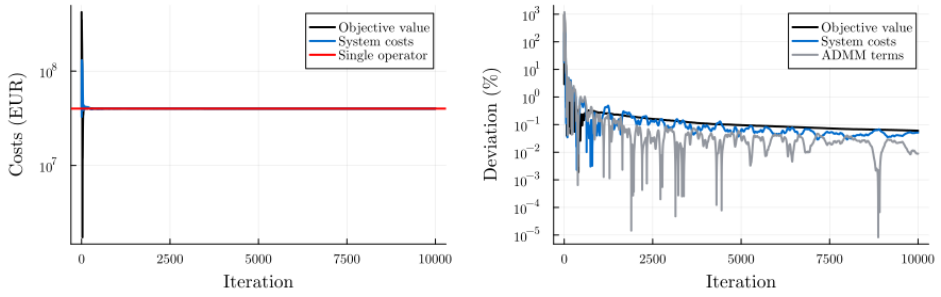

Figure 4: Convergence of the objective value: incl. ADMM terms (black), system costs (excl. ADMM terms), and ADMM terms when compared to the reference value of the single operator.

problem is the objective value and its deviation from the reference provided by the single operator formulation, see Fig. 4. When excluding the ADMM-related terms, the objective value exclusively depicts the system costs. For a sufficiently large number of iterations, the ADMM-related terms should vanish, thus indicating convergence. On the right side in Fig. 4, the objective value is therefore depicted including and excluding the ADMM terms, as well as the deviation between both, i.e., the ADMM terms. All three fall below 1% of the central planner benchmark value after approx. 750 iterations. After 1,500 iterations, the ADMM-related terms become smaller

Table 4: Dispatch (in GWh) per technology at 10,000 iterations, for the single operator problem (SO) and the distributed market-clearing (ADMM), including deviations.

Sector	**Technology**	**Dispatch (in GWh)**		**Deviation**	
		SO	ADMM	Abs. (in GWh)	Rel. (in %)
Electricity	GFPP	236.88	236.83	-0.05	-0.02
	Wind & PV	105.38	105.38	-	-
	Hydro ROR	15.10	15.10	-	-
	CHP	56.84	56.84	-	0.01
	Demand	412.34	412.34	-	-
	PtH	1.85	1.86	-	0.26
Heat	PtH	1.85	1.86	-	0.26
	CHP	23.91	23.91	-	-0.01
	Heat Only	2.26	2.26	-	-
	Demand	7.48	7.48	-	-
	Const. Demand	20.55	20.55	-	-

than 0.1%, while it takes until iteration 6,000 for the objective and cost to fall below 0.1%. While such a gap is sufficiently small for most applications, further assessments are required to determine the convergence properties regarding the primal and dual variables. Furthermore, it has to be remembered that the single-operator problem would not be available for a practical application. Therefore it is crucial to identify other measures that indicate convergence reliably.

In the next step, the quantities of energy supply and demand for different technologies are computed to evaluate the convergence of the dispatch, cf. Tab. 4. After 10,000 iterations, the absolute and relative deviations in the dispatch also become sufficiently small. Solely gas-fired power plants (GFPPs) and the cross-sectoral units, i.e., CHP and power to heat (PtH) units, have observable relative deviations, yet not exceeding 0.26%. In this context, GFPP and CHP units substitute one another due to similar technical constraints and similar costs. The reduced dispatch of CHP units is then compensated by PtH units. Despite the small differences in dispatch, there are gradually higher deviations observable for revenues of suppliers and costs of consumers (in T€) per technology, cf. Tab. 5. Considering the distributed market-clearing, the substitution of electricity generation of CHP units by GFPP leads to considerably smaller deviations in revenues compared to the deviations of renewables, i.e., wind, PV, and hydro. Here, consumers in the

Table 5: Revenue and costs (in T€) per technology at 10,000 iterations in the single operator problem (SO) and in the distributed market-clearing (ADMM) with absolute and relative deviation.

Sector	**Technology**	**Revenues/Costs (in T€)**		**Deviation**	
		SO	ADMM	Abs. (in T€)	Rel. (in %)
Electricity	GFPP	31,598.9	31,676.4	77.5	0.25
	Wind & PV	13,926.6	13,762.1	-164.5	-1.18
	Hydro ROR	1,992.7	2,009.0	16.3	0.82
	CHP	8,489.1	8,499.8	10.7	0.13
	Demand	55,780.8	55,776.8	-4.0	-0.01
	PtH	256.5	258.4	1.9	0.75
Heat	PtH	262.5	264.6	2.1	0.80
	CHP	1,669.8	1,661.8	-8.1	-0.48
	Heat Only	185.2	185.2	-	-
	Demand	445.9	441.2	-4.7	-1.05
	Const. Dem.	1,671.6	1,669.9	-1.7	-0.10

electricity and heat sector are paying slightly less in the distributed market-clearing, while some cross-sectoral technologies, especially PtH units, face higher procurement costs but also achieve higher revenues.

The convergence of the primal and dual root-mean-square deviations (RMSDs) depicted in Figure 5, is a pivotal indicator for the performance of the iterative coordination process.[11] Two main observations are noteworthy in the plots. Firstly, there is a pronounced decrease in RMSD within the initial 1,000 iterations, after which the decline becomes more gradual. Secondly, despite some fluctuations, the curves for both primal and dual RMSDs maintain a negative slope throughout the entire coordination process, indicating continuous improvement. Regarding the fluctuations of primal and dual RMSDs, the variability seems to depend on the technology. For instance, the RMSDs associated with cross-sectoral units, i.e., PtH and CHP, and renewables, i.e., wind, PV and hydro, exhibit comparatively higher fluctuations than those observed for network-coupling RMSD metrics, i.e., for

[11] The RMSD, detailed in Appendix D, is measured in degrees (°) for nodal angles and in MWh for all other variables.

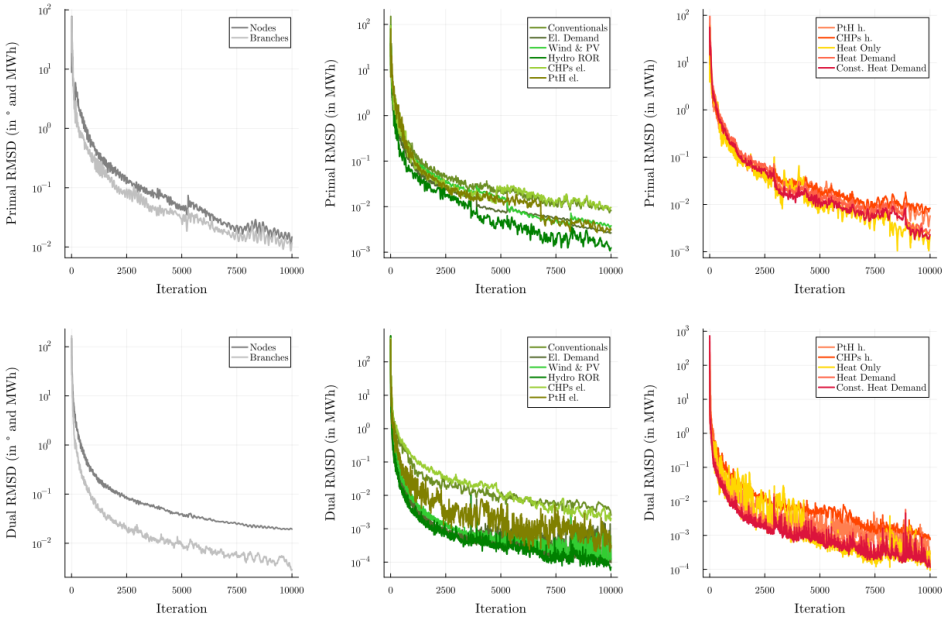

Figure 5: Primal and dual RMSD for networks coupling variables, electricity units and heat units.

nodes and branches. Additionally, the RMSD volatility is more substantial within the heat regions than for the electric sector. It can be observed that the primal and dual RMSD values of all network-coupling variables and technologies fall below, or approach, the 10^{-2} threshold by approximately 10,000 iterations. Correspondingly, primal and dual RMSDs can be considered reasonable metrics for assessing convergence.

4.2.1. Coordination between networks

In this section, light is shed on network-coupling and intra-sectoral coordination aspects, including the convergence. In this context, Fig. 6 depicts the absolute value of the average imbalance of supply and demand in the electricity and heat sector per time-step (in MWh) on the left side. On the right side, absolute deviations in the sum of all transfer payments (in €) are indicated. These metrics can be considered as additional metrics for convergence. A general requirement for a distributed coordination framework in this context is the adequacy of supply and demand, hence, any resulting imbalance should be small to ensure a feasible network operation. Furthermore, any deviations of transfer payments between networks should become small with more iterations, to ensure revenue adequacy in the financial settlement process of networks. In this context, the imbalance in the heat sector declines steadily to values below 1 MWh per time-step, for all 74 heat regions. Meanwhile, the imbalance in the electricity sector decreases only moderately, reaching levels below 10 MWh per time-step after 10,000 iterations. Compared to the 69 GWh of average hourly electricity consumption, this imbalance is yet rather negligible. Even though the deviation of

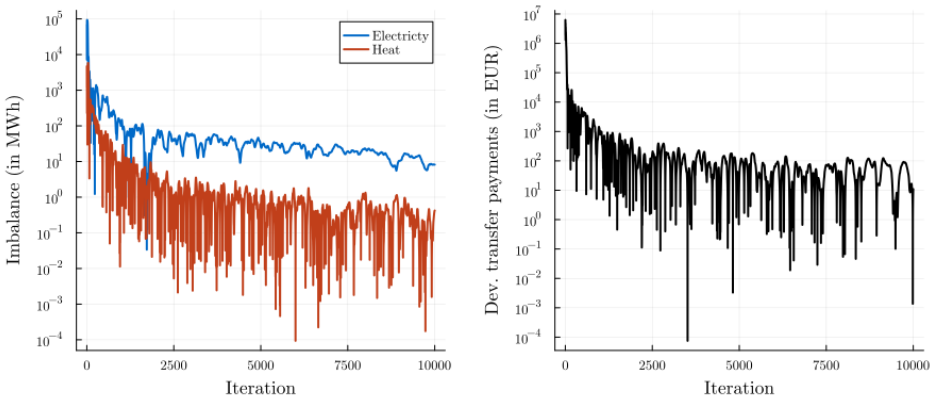

Figure 6: Imbalance - Power heat and revenues.

Table 6: Financial settlement per network (in T€) at iteration 10,000: Revenues, costs, transfer payments, merchant surplus, congestion rent and remaining difference.

Network		Revenues	Costs	Transfer payment	Merchant surplus	Cong. rent	Diff.
Transm.	1	20,816.5	15,919.7	4,896.5	0.3	-	0.3
	2	10,830.8	12,085.5	-1,275.4	20.6	-	20.6
	3	14,606.0	17,950.6	-3,381.6	37.0	35.5	1.5
	4	9,139.6	7,504.8	1,633.6	1.2	-	1.2
Distrib.	1	62.0	0.6	59.7	1.7	0.6	1.1
	2	293.7	484.7	-194.2	3.2	0.9	2.3
	3	43.0	82.8	-40.9	1.1	0.1	1.0
	4	204.4	1,901.8	-1,718.9	21.6	0.1	21.5
	5	38.9	16.7	21.2	1.0	0.2	0.8
Total		**56,035**	**55,947**	**0.1**	**87.8**	**37.3**	**50.5**

transfer payments appears to oscillate steadily between approximately 0.1 and 100 € after iteration 5,000, the financial impact is limited compared to the individual transfer payments as analyzed below.

Especially when considering multiple interconnected networks in the same sector, transfer payments are required to balance the networks' procurement costs of energy and revenues of selling energy. Here, Tab. 6 gives an overview on the financial settlement of networks (in T€). In this context, the merchant surplus is defined as the revenues less costs and transfer payments. In theory, the merchant surplus should be equal to the congestion rent. However, due to the asymptotic nature of convergence of ADMM, differences might occur, which are stated in the last column of Tab. 6. A positive finding is that the distributed coordination framework achieves revenue adequacy for all networks, i.e., there are no negative merchant surpluses for any network. Although these surpluses (summing up to 87.8 T€) surpass the congestion rents of 37.3 T€ by far, this inaccuracy only corresponds to 0.09% of the total costs and revenues. In this context, Fig. 7 depicts the convergence of absolute transfer payments between transmission and distribution networks. While those transfer payments vary widely before 2,500 iterations, thereupon the values stabilize, and the procedure is capable of effectively reducing volatility until iteration 7,500. Thereafter, the convergence enters a less volatile phase of slight adjustments until iteration 10,000.

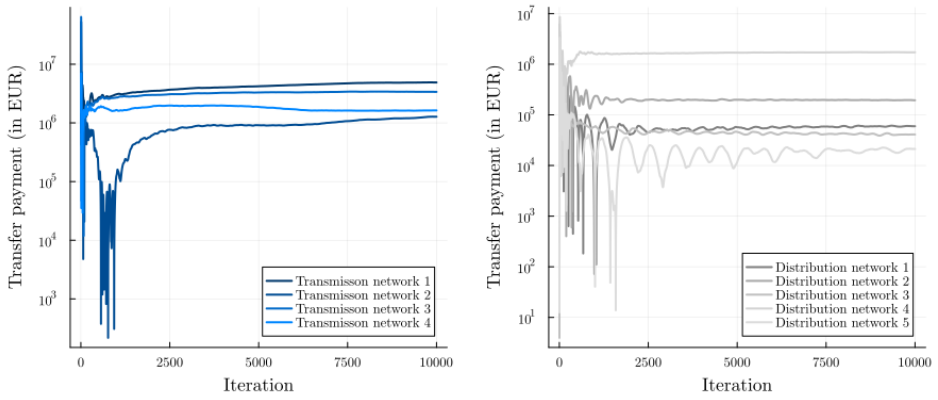

Figure 7: Convergence of absolute transfer payments for transmission and distribution networks.

4.2.2. Computation time

In the following, the computation time of the case study is assessed. In this context, it is noteworthy that the demonstration implementation is based on a sequential computation instead of a full-fledged parallelization, using a single computer with an Intel® Core™ i9-9900K CPU @ 3.60GHz and 128 GB RAM. Here, the computation times of the individual subproblems per iteration were tracked, cf. Figure 8, thus, allowing to shed light on possible computation times in case of a parallelization. In our application, solving the electricity (transmission and distribution) network subproblems often takes the most time, i.e., between 0.09 and 0.79 s, followed by the units' subproblem with 0.19 to 0.53 s. The heat networks range between 0.01 and 0.10 ms. In the implementation, all units were co-optimized in one subproblem, despite their independence and separability. Similarly, all 74 heat networks were co-optimized—despite their separability. For 10,000 iterations, this parallel computation of networks and units would take 1.59 hours. This benchmark assumes that the slowest computation time of all agents per iteration limits the performance.[12] A key advantage of the proposed framework is relevant: the full models must be built only once, as is in general the case with ADMM. Despite the numerical calculations of the coordination step and the price updates, exclusively the objective function of the corresponding subproblems needs updating, thus, saving a significant amount of time for large-scale applications. The application of ADMM in

[12]Neglecting any possible communication efforts.

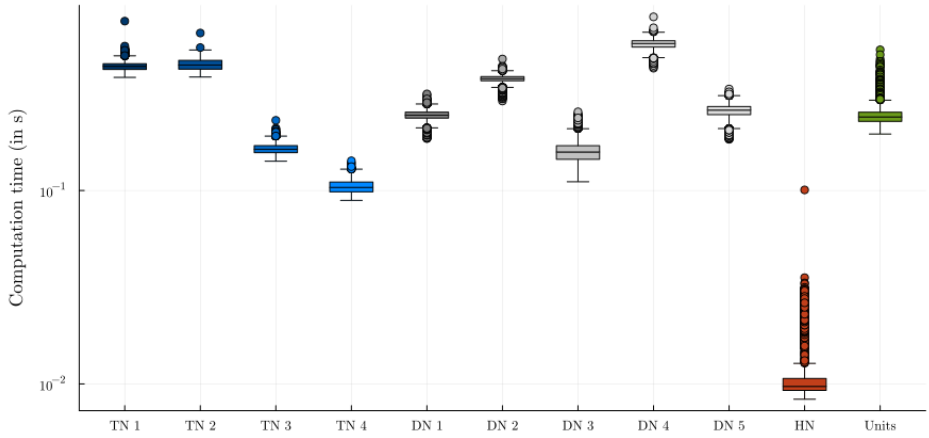

Figure 8: Computation time per iteration of transmission networks (TN), distribution network (DN), heat networks (HN), and units.

this paper, where the slowest agent limits the overall performance, is called synchronous ADMM, cf. Zhang and Kwok (2014). Here, an asynchronous application of ADMM could potentially reduce processing times even further and yield accelerations, as discussed in Zhang and Kwok (2014).

Regarding parallelization efforts, there are two leverages: First, it is noteworthy that for electricity networks, there are no inter-temporal constraints, cf. Appendix E. Therefore, by optimizing each time-step in parallel, the electricity networks would be able to cut computation time substantially. Second, replacing the previously mentioned co-optimization of heat networks and units with a parallelization of individual subproblems seems promising as well. Consequently, the computation time per individual unit and heat network could be reduced significantly when optimized entirely in parallel. Taking advantage of these potentials, a fully parallel computation of networks and units (applying synchronous ADMM) in a distributed setting could potentially lift computation times to approx. 15.9 minutes[13]. However, it is important to note that communication speed will play a crucial role in achieving this efficiency, especially with 10,000 iterations.

[13]Presuming a linear decrease in computation times of electricity networks by the number of considered time-steps (i.e., here six hours with an hourly resolution) and a substantial decrease of processing times for individual unit subproblems.

5. Conclusion

In this paper, a novel distributed coordination framework is introduced, enabling a cross-sectoral multi-operator market-clearing framework, where autonomous agents such as unit and network operators engage in distributed communication solely with their directly connected neighbors. This approach, based on ADMM, maintains manageable problem sizes for individual agents and integrates cross-sectoral and network-coupling coordination efficiently. It also ensures the confidentiality of sensitive economic data, while its scalability and tractability for large-scale applications are promising. A large-scale case study of a cross-sectoral and inter-temporal energy system in Germany under a decarbonized scenario was carried out. The effectiveness and reliability of the proposed method were demonstrated from both a technical and economic perspective. This simultaneous coordination framework reaches equivalent results as a single-operator framework, and it enables market-driven incentives for efficient resource utilization while avoiding the risks of inefficient dispatches inherent to sequential approaches.

The results of the case study indicate that the primal and dual variables can be interpreted properly both in technical and economic terms. The multiplication of both primal and dual variables yields revenues, costs, and transfer payments that are required in the financial settlement process to value the exchanged energy at interconnections between multiple networks and any interconnected unit. In the considered case study, revenue adequacy was observed for all networks and cost recovery for all units. However, the case study showed that the financial settlement requires more iterations to achieve converging results than the dispatch decisions. A series of potential indicators and metrics for convergence were introduced and assessed.

Regarding future work, implementational aspects for real-world applications are worth consideration. Especially, a full-fledged parallelization of all subproblems to minimize computation times seems to be promising. Furthermore, the introduction of initial values for dual and primal variables, as part of a potential model warm-start, together with other acceleration techniques could also improve the framework's convergence.

Declaration of generative AI and AI-assisted technologies in the writing process

While preparing this work, the author used ChatGPT and Grammarly to improve the language and readability of selected parts of the manuscript. After using these tools, the author carefully reviewed and edited the content as needed, taking full responsibility for the content of the publication.

References

Bouckaert, S., Fernandez Pales, A., McGlade, C., Remme, U., Wanner, B., Varro, L., D'Ambrosio, D., Spencer, T., 2021. Net Zero by 2050: A Roadmap for the Global Energy Sector. Technical Report. International Energy Agency.

Boyd, S., Parikh, N., Chu, E., Peleato, B., Eckstein, J., et al., 2011. Distributed optimization and statistical learning via the alternating direction method of multipliers. Foundations and Trends® in Machine learning 3, 1–122.

Chatzipanagiotis, N., Dentcheva, D., Zavlanos, M.M., 2015. An augmented lagrangian method for distributed optimization. Mathematical Programming 152, 405–434.

Chen, C., He, B., Ye, Y., Yuan, X., 2016. The direct extension of admm for multi-block convex minimization problems is not necessarily convergent. Mathematical Programming 155, 57–79.

Chen, S., Conejo, A.J., Wei, Z., 2021. Gas-power coordination: from day-ahead scheduling to actual operation. IEEE Transactions on Power Systems 37, 1532–1542.

Chen, Y., Wei, W., Liu, F., Wu, Q., Mei, S., 2018. Analyzing and validating the economic efficiency of managing a cluster of energy hubs in multi-carrier energy systems. Applied energy 230, 403–416.

Dall'Anese, E., Mancarella, P., Monti, A., 2017. Unlocking flexibility: Integrated optimization and control of multienergy systems. IEEE Power and Energy Magazine 15, 43–52.

Deng, W., Lai, M.J., Peng, Z., Yin, W., 2014. Parallel multi-block admm with o (1/k) convergence. arXiv preprint arXiv:1312.3040 .

Deutsche Energie-Agentur GmbH, 2018. dena-Leitstudie Integrierte Energiewende: Impulse für die Gestaltung des Energiesystems bis 2050. Technical Report. Deutsche Energie-Agentur GmbH. Berlin.

Ding, T., Jia, W., Shahidehpour, M., Han, O., Sun, Y., Zhang, Z., 2022. Review of optimization methods for energy hub planning, operation, trading, and control. IEEE Transactions on Sustainable Energy 13, 1802–1818.

EU Parliament and EU Council, 2019. EU 2019/943 - regulation on the internal market for electricity.

EU Parliament and EU Council, 2022. EU 2022/2557 - directive on the resilience of critical entities and repealing council directive 2008/114/ec.

Felten, B., 2020. An integrated model of coupled heat and power sectors for large-scale energy system analyses. Applied Energy 266, 114521.

Felten, B., Osinski, P., Felling, T., Weber, C., 2021. The flow-based market coupling domain-why we can't get it right. Utilities Policy 70, 101136.

Grimm, V., Martin, A., Sölch, C., Weibelzahl, M., Zöttl, G., 2022. Market-based redispatch may result in inefficient dispatch. The Energy Journal 43, 205–230.

He, C., Zhang, X., Liu, T., Wu, L., Shahidehpour, M., 2018a. Coordination of interdependent electricity grid and natural gas network—a review. Current Sustainable/Renewable Energy Reports 5, 23–36.

He, Y., Yan, M., Shahidehpour, M., Li, Z., Guo, C., Wu, L., Ding, Y., 2018b. Decentralized optimization of multi-area electricity-natural gas flows based on cone reformulation. IEEE Transactions on Power Systems 33, 4531–4542.

Hirth, L., Schlecht, I., et al., 2019. Market-based redispatch in zonal electricity markets: Inc-dec gaming as a consequence of inconsistent power market design (not market power). Working Paper .

Hogan, W.W., 1998. Independent system operator: Pricing and flexibility in a competitive electricity market. Center for Business and Government, JF Kennedy School of Government, Harvard University, MA .

Hogan, W.W., 2021. Electricity market design: Multi-interval pricing models. Harvard University .

Hogan, W.W., 2022. Electricity market design and zero-marginal cost generation. Current Sustainable/Renewable Energy Reports 9, 15–26.

Javadi, M.S., Nezhad, A.E., Jordehi, A.R., Gough, M., Santos, S.F., Catalão, J.P., 2022. Transactive energy framework in multi-carrier energy hubs: A fully decentralized model. Energy 238, 121717.

Jimenez-Navarro, J.P., Kavvadias, K., Filippidou, F., Pavičević, M., Quoilin, S., 2020. Coupling the heating and power sectors: The role of centralised combined heat and power plants and district heat in a european decarbonised power system. Applied Energy 270, 115134.

Kavulla, T., 2019. Efficient solutions for issues in electricity seams. Technical Report. R Street Institute.

Khorasany, M., Mishra, Y., Ledwich, G., 2018. Market framework for local energy trading: A review of potential designs and market clearing approaches. IET Generation, Transmission & Distribution 12, 5899–5908.

Krueger, C., Otte, M., Holly, S., Rathjen, S., Wellssow, A., Lehnhoff, S., 2023. Redispatch 3.0–congestion management for german power grids–considering controllable resources in low-voltage grids, in: ETG Congress 2023, VDE. pp. 1–7.

Küfeoglu, S., Liu, G., Anaya, K., Pollitt, M., 2019. Digitalisation and new business models in energy sector. EPRG Working Paper, Cambridge Working Paper in Economics .

Litvinov, E., Zhao, F., Zheng, T., 2019. Electricity markets in the united states: Power industry restructuring processes for the present and future. IEEE Power and Energy Magazine 17, 32–42.

Molzahn, D.K., Dörfler, F., Sandberg, H., Low, S.H., Chakrabarti, S., Baldick, R., Lavaei, J., 2017. A survey of distributed optimization and control algorithms for electric power systems. IEEE Transactions on Smart Grid 8, 2941–2962.

Mühlpfordt, T., Dai, X., Engelmann, A., Hagenmeyer, V., 2021. Distributed power flow and distributed optimization—formulation, solution, and open source implementation. Sustainable Energy, Grids and Networks 26, 100471.

Pinson, P., 2023. What may future electricity markets look like? Journal of Modern Power Systems and Clean Energy .

Radecke, J., Hefele, J., Hirth, L., 2019. Markets for local flexibility in distribution networks.

Ryu, E.K., Yin, W., 2022. Large-Scale Convex Optimization: Algorithms & Analyses via Monotone Operators. Cambridge University Press.

Schinke-Nendza, A., Conejo, A., Weber, C., 2024a. A distributed market-clearing framework for highly interconnected electricity and gas systems. Preprint at SSRN .

Schinke-Nendza, A., Kramer, H., Khalid, A., Flatter, F., Rasti, S., Uhlemeyer, B., Weber, C., 2024b. Modeling of large decentral multi-energy systems: An application to flexible heat pumps in a decarbonized scenario. Preprint at TechRxiv .

Sorin, E., Bobo, L., Pinson, P., 2018. Consensus-based approach to peer-to-peer electricity markets with product differentiation. IEEE Transactions on Power Systems 34, 994–1004.

Stute, J., Kühnbach, M., 2023. Dynamic pricing and the flexible consumer–investigating grid and financial implications: A case study for germany. Energy Strategy Reviews 45, 100987.

Wang, H., Banerjee, A., Luo, Z.Q., 2014. Parallel direction method of multipliers. Advances in Neural Information Processing Systems 27.

Wang, Y., Wu, L., Wang, S., 2016. A fully-decentralized consensus-based admm approach for dc-opf with demand response. IEEE Transactions on Smart Grid 8, 2637–2647.

Weber, C., 2023. Achievements and challenges in european energy markets. Journal of Modern Power Systems and Clean Energy 11, 698–704.

Weber, C., Möst, D., Fichtner, W., 2022. Economics of power systems: Fundamentals for sustainable energy. Springer Nature.

Wu, G., Xiang, Y., Liu, J., Gou, J., Shen, X., Huang, Y., Jawad, S., 2020. Decentralized day-ahead scheduling of multi-area integrated electricity and natural gas systems considering reserve optimization. Energy 198, 117271.

Yang, Y., Guan, X., Jia, Q.S., Yu, L., Xu, B., Spanos, C.J., 2022. A survey of admm variants for distributed optimization: Problems, algorithms and features. arXiv preprint arXiv:2208.03700 .

Zhang, R., Kwok, J., 2014. Asynchronous distributed admm for consensus optimization, in: International conference on machine learning, PMLR. pp. 1701–1709.

Appendix

A. Equivalence of the general problem and the decomposed problem

Considering the single operator problem (1), the coupling constraints interrelating networks and units as well as different networks, i.e., Eq. (1b), prevent a decomposition of the problem that would lead to a parallelizable implementation structure. Specifically, applying ADMM directly to the problem results in primal updates that do not allow for independent computation despite the multi-block nature of the problem, cf. Section 2.4. To circumvent this challenge, a two-fold modification is applied to problem (1) to facilitate a distributed computational framework, thereby enabling the efficient application of ADMM. We start by reformulating the overarching coupling constraint (1b) into separable *bilateral coupling constraints* that connect individual units to networks and also establish pairwise connections between networks. Subsequently, a *coordination step* is introduced, designed to segregate the intertwined network and unit subproblems, thereby allowing for a distributed architecture that supports fully parallel processing of unit and network subproblems. This approach not only enhances computational efficiency and reduces communication efforts but also elucidates the market-clearing mechanism, offering a clear and intuitive understanding.

Bilateral coupling constraints: To obtain *bilateral coupling constraints*, for a given network $k \in \mathcal{K}^e$ in sector $e \in \mathcal{E}$ auxiliary variables $\boldsymbol{\zeta}^N_{k,n}$ for network-related variables and $\boldsymbol{\zeta}^U_{k,i}$ for unit-related variables are introduced. Thereupon, the coupling constraint, i.e., Eq. (1b), can be reformulated as follows for all networks $k \in \mathcal{K}^e$ in sector $e \in \mathcal{E}$

$$\widetilde{\boldsymbol{z}}_{n,k} = \boldsymbol{\zeta}^N_{k,n} \quad : \boldsymbol{\lambda}^N_{k,n}, \qquad \forall n \in \mathcal{K}^e \setminus \{k\}, \tag{18a}$$

$$\widetilde{\boldsymbol{x}}_{i,k} = \boldsymbol{\zeta}^U_{k,i} \quad : \boldsymbol{\lambda}^U_{k,i}, \qquad \forall i \in \mathcal{I}, \tag{18b}$$

$$\sum_{i \in \mathcal{I}} \boldsymbol{A}^U_{i,k} \boldsymbol{\zeta}^U_{k,i} + \sum_{n \in \mathcal{K}^e \setminus \{k\}} \boldsymbol{A}^N_{n,k} \boldsymbol{\zeta}^N_{k,n} + \boldsymbol{B}^N_k \widetilde{\boldsymbol{z}}_k = \boldsymbol{C}^N_k \quad : \boldsymbol{\lambda}_k, \tag{18c}$$

whereby the indices in the subscript of the variables indicate the variables' assignment and interconnection: the first index indicates the entity to which

the variable is *assigned*, while the second index defines the entity to which the variable establishes a *connection*. These auxiliary variables $\{\boldsymbol{\zeta}^N_{k,n}, \boldsymbol{\zeta}^U_{k,i}\} \subseteq \boldsymbol{\zeta}_k$ are assigned to network operator k and constraint (18c) to the feasibility set of network operator k, previously defined in Eq. (1c). The relationship of the networks' variables $\boldsymbol{z}_k$ and $\boldsymbol{\zeta}_k$ to the new feasibility set (denoted as $\mathcal{Z}^\zeta_k$) is then defined as

$$\boldsymbol{z}_k, \boldsymbol{\zeta}_k \in \mathcal{Z}^\zeta_k, \qquad \forall k \in \mathcal{K}^e, e \in \mathcal{E}, \tag{19}$$

thus, replacing constraint (1c), together with constraints (18a) and (18b). It is trivial to show that $\boldsymbol{\lambda}^N_{k,n}$ and $\boldsymbol{\lambda}^U_{k,i}$ are equal to either the value of $\boldsymbol{\lambda}_k$ or to its negative counterpart, as Eq. (18a) and (18b) establish ordinary equality constraints that are directly linked to the nodal balancing constraint (1b), thus to the LMPs of network k in sector e.

Coordination step: We now introduce variables that are required for a *coordination step* to obtain a fully parallelizable structure. For the networks, auxiliary variables $\boldsymbol{\psi}^{N,src}_{n,k}$ and $\boldsymbol{\psi}^{N,dest}_{k,n}$, are introduced which are assigned to the coordination step. Here, index *src* references the source network, and index *dest* references the destination network to which the balancing constraint is assigned. Consequently, the network-connecting bilateral coupling constraint, i.e., Eq. (18a), are formulated as follows

$$\widetilde{\boldsymbol{z}}_{n,k} = \boldsymbol{\psi}^{N,src}_{n,k}, \qquad : \boldsymbol{\lambda}^{N,src}_{k,n}, \qquad \forall k \in \mathcal{K}^e, n \in \mathcal{K}^e \setminus \{k\} \in \mathcal{E}, \tag{20a}$$

$$\boldsymbol{\zeta}^N_{k,n} = \boldsymbol{\psi}^{N,dest}_{k,n}, \qquad : \boldsymbol{\lambda}^{N,dest}_{k,n}, \qquad \forall k \in \mathcal{K}^e, n \in \mathcal{K}^e \setminus \{k\} \in \mathcal{E}, \tag{20b}$$

$$\boldsymbol{\psi}^{N,src}_{n,k} = \boldsymbol{\psi}^{N,dest}_{k,n}, \qquad : \boldsymbol{\lambda}^{N}_{k,n}, \qquad \forall k \in \mathcal{K}^e, n \in \mathcal{K}^e \setminus \{k\} \in \mathcal{E}, \tag{20c}$$

where $\boldsymbol{\lambda}^{N,src}_{k,n}$ and $\boldsymbol{\lambda}^{N,dest}_{k,n}$ are equal to positive or negative values of $\boldsymbol{\lambda}^N_{k,n}$, as Eq. (20a) to (20c) establish ordinary equality constraints.

Similarly, auxiliary variables $\boldsymbol{\psi}^{U,src}_{i,k}$ and $\boldsymbol{\psi}^{U,dest}_{k,i}$ are introduced for units, which are then assigned to the coordination step. Here, index *src* references the source, i.e., the unit, and index *dest* references the destination network to which the balancing constraint is assigned. Consequently, the network-unit-connecting bilateral coupling constraints, i.e., Eq. (18b), can be reformulated as follows

$$\widetilde{\boldsymbol{x}}_{i,k} = \boldsymbol{\psi}^{U,src}_{i,k}, \qquad : \boldsymbol{\lambda}^{U,src}_{k,i}, \qquad \forall i \in \mathcal{I}, k \in \mathcal{K}^e, e \in \mathcal{E}, \tag{21a}$$

$$\boldsymbol{\zeta}^U_{k,i} = \boldsymbol{\psi}^{U,dest}_{k,i}, \qquad : \boldsymbol{\lambda}^{U,dest}_{k,i}, \qquad \forall i \in \mathcal{I}, k \in \mathcal{K}^e, e \in \mathcal{E}, \tag{21b}$$

$$\boldsymbol{\psi}^{U,src}_{i,k} = \boldsymbol{\psi}^{U,dest}_{k,i}, \qquad : \boldsymbol{\lambda}^{U}_{k,i}, \qquad \forall i \in \mathcal{I}, k \in \mathcal{K}^e, e \in \mathcal{E}, \tag{21c}$$

where $\boldsymbol{\lambda}_{k,i}^{U,src}$ and $\boldsymbol{\lambda}_{k,i}^{U,dest}$ are equivalent to $\boldsymbol{\lambda}_{k,i}^{U}$, as Eq. (21a) to (21c) establish ordinary equality constraints. Therefore, the single operator problem (1) can be rewritten equivalently as

$$\min_{\boldsymbol{x},\boldsymbol{z}} \quad \sum_{i\in\mathcal{I}} f_i\left(\boldsymbol{x}_i\right) + \sum_{e\in\mathcal{E}}\sum_{k\in\mathcal{K}^e} g_k\left(\boldsymbol{z}_k\right) \tag{22a}$$

$$\text{s.t.} \quad \widetilde{\boldsymbol{z}}_{n,k} = \boldsymbol{\psi}_{n,k}^{N,src} \quad : \boldsymbol{\lambda}_{k,n}^{N,src}, \quad \forall n \in \mathcal{K}^e \setminus \{k\}, k \in \mathcal{K}^e, e \in \mathcal{E}, \tag{22b}$$

$$\boldsymbol{\zeta}_{k,n}^{N} = \boldsymbol{\psi}_{k,n}^{N,dest} \quad : \boldsymbol{\lambda}_{k,n}^{N,dest}, \quad \forall n \in \mathcal{K}^e \setminus \{k\}, k \in \mathcal{K}^e, e \in \mathcal{E}, \tag{22c}$$

$$\boldsymbol{\psi}_{n,k}^{N,src} = \boldsymbol{\psi}_{k,n}^{N,dest} \quad : \boldsymbol{\lambda}_{k,n}^{N}, \quad \forall n \in \mathcal{K}^e \setminus \{k\}, k \in \mathcal{K}^e, e \in \mathcal{E}, \tag{22d}$$

$$\widetilde{\boldsymbol{x}}_{i,k} = \boldsymbol{\psi}_{i,k}^{U,src}, \quad : \boldsymbol{\lambda}_{k,i}^{U,src}, \quad \forall i \in \mathcal{I}, k \in \mathcal{K}^e, e \in \mathcal{E}, \tag{22e}$$

$$\boldsymbol{\zeta}_{k,i}^{U} = \boldsymbol{\psi}_{k,i}^{U,dest}, \quad : \boldsymbol{\lambda}_{k,i}^{U,dest}, \quad \forall i \in \mathcal{I}, k \in \mathcal{K}^e, e \in \mathcal{E}, \tag{22f}$$

$$\boldsymbol{\psi}_{i,k}^{U,src} = \boldsymbol{\psi}_{k,i}^{U,dest}, \quad : \boldsymbol{\lambda}_{k,i}^{U}, \quad \forall i \in \mathcal{I}, k \in \mathcal{K}^e, e \in \mathcal{E}, \tag{22g}$$

$$\boldsymbol{z}_k, \boldsymbol{\zeta}_k \in \mathcal{Z}_k^{\zeta}, \quad \forall k \in \mathcal{K}^e, e \in \mathcal{E}, \tag{22h}$$

$$\boldsymbol{x}_i \in \mathcal{X}_i, \quad \forall i \in \mathcal{I}. \tag{22i}$$

With respect to decomposition, the coupling in problem (22) now consists of bilateral equality constraints exclusively, with variables $\{\widetilde{\boldsymbol{x}}_{i,k}, \boldsymbol{x}_i\} \subseteq \boldsymbol{x}$ being assigned to units, variables $\{\boldsymbol{z}_k, \widetilde{\boldsymbol{z}}_{n,k}, \boldsymbol{\zeta}_k\} \subseteq \boldsymbol{z}$ being assigned to networks, and variables $\left\{\boldsymbol{\psi}_{n,k}^{N,src}, \boldsymbol{\psi}_{k,n}^{N,dest}, \boldsymbol{\psi}_{i,k}^{U,src}, \boldsymbol{\psi}_{k,i}^{U,dest}\right\} \subseteq \boldsymbol{\psi}_k^e$ being assigned to the coordination step.

Considering problem (22), now ADMM can be applied to obtain a fully distributed iterative coordination framework with autonomous agents, i.e., network and unit operators, that are capable of optimizing themselves completely in parallel. In this setup, communication is exclusively required between interconnected agents, i.e., units and networks, or between two networks, once per iteration.

B. Coupling constraints between electricity networks

In the following, the case of multiple interconnected transmission and distribution networks in the electricity sector is considered. Regarding the coupling constraints, nodal and branch-related variables can be distinguished, i.e., the voltage angles θ_n and power flows p_m^F in the case of a DC-power flow.[14] A common approach to obtain a distributed power flow is a decomposition establishing equality constraints on a nodal level exclusively, i.e.,

[14] For sake of simplicity the time-index t is disregarded here.

using voltage angles in the case of a DC-power flow, cf. Wang et al. (2016), and also voltage magnitudes in the case of an AC-PF, cf. Mühlpfordt et al. (2021). While exchanging additional, redundant information (e.g., on the power flow) is technically unnecessary, it proves beneficial to share extra information on power flow. Hence, for any branch m connecting two nodes n_1 and n_2, which are assigned to two different networks, information on the three variables is exchanged, i.e., $\theta_{n_1}, \theta_{n_2}$ and p_m^F, where branch $m \in \mathcal{M}_{AC}$ connects nodes $n_1, n_2 \in \mathcal{N}$. The reformulation and decomposition is depicted in Fig. 9, for an exemplary interconnection between two networks.

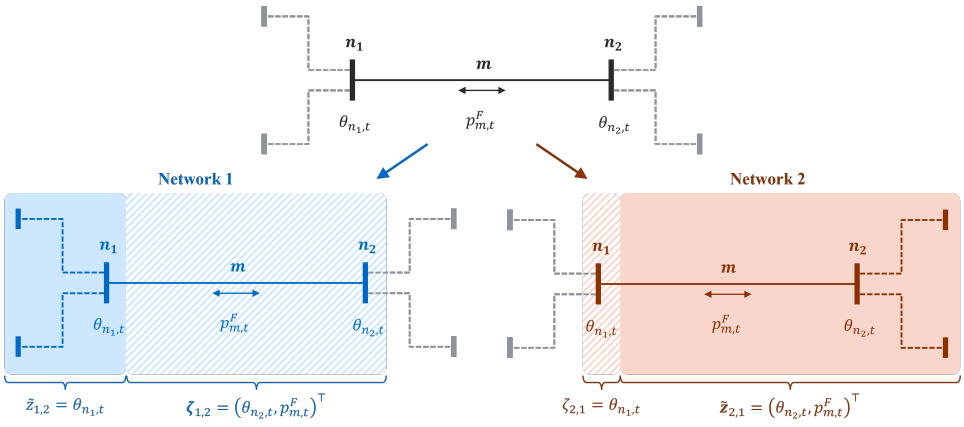

Figure 9: Exemplary interconnection between two networks.

Here, it is important that constraint duplications within the subproblems of the networks have to be avoided. Hence, the connecting line should be assigned exclusively to one subsystem (network), which then enforces inequality constraints, notably the maximum line capacity $p_m^{F,+}$. Any duplication of inequality constraints would affect dual variables, congestion rents, and, thus, the transfer payments, cf. Appendix C. Thereupon, the variables of the original problem can be reformulated and auxiliary variables ψ can be introduced, leading to an asymmetrical definition of auxiliary variables. In the given example of Fig. 9, the transmission line is assigned to network 2. Therefore, network 1 introduces auxiliary variables for the power flow p_m^F across the transmission line and for the voltage angle θ_{n_2} of node n_2 in network 2. This is indicated by the blue hatched area in network 1 (i.e., on the lower left side of Fig. 9). Consequently, network 2 introduces an auxiliary variable for the voltage angle θ_{n_1} of node n_1 in network 1—as indicated by the red hatched area in network 2 (i.e., on the lower right side of Fig. 9).

For the sake of simplicity, the time index t is neglected in the following. The variables of network 1 then follow as

$$\widetilde{z}_{2,1} = \theta_{n_1}, \tag{23a}$$

$$\boldsymbol{\zeta}_{1,2} = \left(\theta_{n_2}, p_m^F\right)^\top, \tag{23b}$$

and the variables of network 2 as

$$\widetilde{\boldsymbol{z}}_{1,2} = \left(\theta_{n_2}, p_m^F\right)^\top, \tag{24a}$$

$$\zeta_{2,1} = \theta_{n_1}. \tag{24b}$$

Introducing the variables assigned to the coordination step yields

$$\widetilde{z}_{2,1} = \psi_{2,1}^{N,src}, \qquad : \lambda_{1,2}^{N,src}, \tag{25a}$$

$$\boldsymbol{\zeta}_{1,2} = \boldsymbol{\psi}_{1,2}^{N,dest}, \qquad : \boldsymbol{\lambda}_{1,2}^{N,dest}, \tag{25b}$$

for network 1 and

$$\widetilde{\boldsymbol{z}}_{1,2} = \boldsymbol{\psi}_{1,2}^{N,src}, \qquad : \boldsymbol{\lambda}_{2,1}^{N,src}, \tag{26a}$$

$$\zeta_{2,1} = \psi_{2,1}^{N,dest}, \qquad : \lambda_{2,1}^{N,dest}, \tag{26b}$$

for network 2. The equality constraints of the corresponding coordination step are then defined as

$$\boldsymbol{\psi}_{1,2}^{N,dest} = \boldsymbol{\psi}_{1,2}^{N,src}, \tag{27a}$$

$$\psi_{2,1}^{N,src} = \psi_{2,1}^{N,dest}. \tag{27b}$$

C. Transfer payments between networks

Considering the distributed market-clearing in a multi-energy system, there is a requirement for *transfer payments* between interconnected networks. These payments ensure that cashflows from and to market participants in the financial settlement add up to the results of the overall market-clearing and that congestion rents are allocated to the corresponding network operator. The payments are determined by the multiplication of dual and primal variables of the coupling constraints between all network operators. For electricity networks represented through a linear power flow approximation (i.e., a DC power flow), transfer payments are based on two coupling constraints: First, the voltage angles at physical interconnections, and second, the power flows across the interconnecting branches.

For the example given in Appendix B, the properties of the introduced auxiliary variables for the interconnecting branch between networks 1 and 2 can be derived for any iteration ν:

- First, based on Eq. (16) it can be concluded that $\lambda_{1,2}^{N,src} = -\lambda_{2,1}^{N,dest}$ and $\boldsymbol{\lambda}_{2,1}^{N,src} = -\boldsymbol{\lambda}_{1,2}^{N,dest}$ must hold.
- Second, the coordination step yields $\boldsymbol{\psi}_{1,2}^{N,dest} = \boldsymbol{\psi}_{1,2}^{N,src}$ and $\psi_{2,1}^{N,src} = \psi_{2,1}^{N,dest}$.

Thereupon, the transfer payments for any iteration ν are defined as

$$\boldsymbol{C}_{1,2}^{N,dest} = \boldsymbol{\psi}_{1,2}^{N,dest} \odot \boldsymbol{\lambda}_{1,2}^{N,dest} \overset{!}{=} -\boldsymbol{\psi}_{1,2}^{N,src} \odot \boldsymbol{\lambda}_{2,1}^{N,src} = -\boldsymbol{C}_{1,2}^{N,src}, \tag{28a}$$

$$C_{2,1}^{N,src} = \psi_{2,1}^{N,src} \cdot \lambda_{1,2}^{N,src} \overset{!}{=} -\psi_{2,1}^{N,dest} \cdot \lambda_{2,1}^{N,dest} = -C_{2,1}^{N,dest}, \tag{28b}$$

with $\odot$ the Hadamard or element-wise product. Then $C_{1,2} = C_{2,1}^{N,src} + \mathbf{1}^\top \boldsymbol{C}_{1,2}^{N,dest}$ defines the transfer payments of network 1 to network 2, which may be positive or (in case of value streams in the opposite direction) negative.[15] Vice versa, $C_{2,1} = C_{2,1}^{N,dest} + \mathbf{1}^\top \boldsymbol{C}_{1,2}^{N,src}$ defines the transfer payments of network 2 to network 1. Here, the relationship $C_{1,2} = -C_{2,1}$ must hold, i.e., the transfer payments paid by one network must be equal to the received transfer payment of the other network.

Taking more complex power flow approximations into account, there might be additional coupling constraints for supplementary variables, e.g., voltage magnitudes, cf. Mühlpfordt et al. (2021). Consequently, there have to be further transfer payments between network operators depending on the dual and primal variables.

D. Residuals and root-mean-square deviations of primals and duals

Primal and dual resdiuals: Regarding the primal and dual residuals of the decomposed subproblems (10) and (11) with the coordination step and dual variable updates (14b) and (15b), first the square sums of primal residuals are defined. For networks and units these *primal residuals* follow as

$$\left\| r^{N,src,\nu} \right\|_2 = \sqrt{\sum_{k \in \mathcal{K}^e} \sum_{n \in \mathcal{K}^e \setminus \{k\}} \left\| \left(\boldsymbol{\psi}_{n,k}^{N,src} \right)^\nu - \left(\widetilde{\boldsymbol{z}}_{n,k} \right)^\nu \right\|_2^2}, \tag{29a}$$

$$\left\| r^{N,dest,\nu} \right\|_2 = \sqrt{\sum_{k \in \mathcal{K}^e} \sum_{n \in \mathcal{K}^e \setminus \{k\}} \left\| \left(\boldsymbol{\psi}_{k,n}^{N,dest} \right)^\nu - \left(\boldsymbol{\zeta}_{k,n}^{N} \right)^\nu \right\|_2^2}, \tag{29b}$$

[15] With $\mathbf{1}^\top = (1, 1)$, here.

$$\left\|r^{U,src,\nu}\right\|_2 = \sqrt{\sum_{k\in\mathcal{K}^e}\sum_{i\in\mathcal{I}}\left\|\left(\boldsymbol{\psi}_{i,k}^{U,src}\right)^{\nu} - \left(\widetilde{\boldsymbol{x}}_{i,k}\right)^{\nu}\right\|_2^2}, \tag{29c}$$

$$\left\|r^{U,dest,\nu}\right\|_2 = \sqrt{\sum_{k\in\mathcal{K}^e}\sum_{i\in\mathcal{I}}\left\|\left(\boldsymbol{\psi}_{k,i}^{U,dest}\right)^{\nu} - \left(\boldsymbol{\zeta}_{k,i}^{U}\right)^{\nu}\right\|_2^2}. \tag{29d}$$

Using the properties of Eq. (12) and (13) together with Eq. (16) yields

$$\left\|r^{N,src,\nu}\right\|_2 = \left\|r^{N,dest,\nu}\right\|_2, \qquad \text{and} \qquad \left\|r^{U,src,\nu}\right\|_2 = \left\|r^{U,dest,\nu}\right\|_2, \tag{30}$$

We can use the properties of the coordination step[16] to define the square sums of *dual residuals* of networks and units as

$$\left\|s^{N,src,\nu}\right\|_2 = \varphi^{\nu}\rho^{\nu}\sqrt{\sum_{k\in\mathcal{K}^e}\sum_{n\in\mathcal{K}^e\setminus\{k\}}\left\|\left(\boldsymbol{\psi}_{n,k}^{N,src}\right)^{\nu} - \left(\boldsymbol{\psi}_{n,k}^{N,src}\right)^{\nu-1}\right\|_2^2}, \tag{31a}$$

$$\left\|s^{U,src,\nu}\right\|_2 = \varphi^{\nu}\rho^{\nu}\sqrt{\sum_{k\in\mathcal{K}^e}\sum_{i\in\mathcal{I}}\left\|\left(\boldsymbol{\psi}_{i,k}^{U,src}\right)^{\nu} - \left(\boldsymbol{\psi}_{i,k}^{U,src}\right)^{\nu-1}\right\|_2^2}, \tag{31b}$$

where $\left\|s^{N,src,\nu}\right\|_2 = \left\|s^{N,dest,\nu}\right\|_2$ and $\left\|s^{U,src,\nu}\right\|_2 = \left\|s^{U,dest,\nu}\right\|_2$ hold.

Primal and dual root-mean-square deviations: To obtain meaningful, problem-size independent indicators for convergence, a simple scaling can be applied: Dividing the primal and dual residuals by the total number of considered instances (i.e., time-steps multiplied by the number of nodes, branches or units per technology), before calculating the square-root, the root-mean-square deviation (RMSD) of the primal and dual variables are derived, cf. Schinke-Nendza et al. (2024a). This leads to a negative-oriented evaluation metric indicating deviations in an aggregated manner on the level of connecting nodes and branches or on a unit-level. We denote the total number of considered instances as K and define the primal RMSDs of networks and units as

$$RMSD_r^{N,e,\nu} = \frac{\left\|r^{N,src,\nu}\right\|_2}{\sqrt{K}}, \qquad \text{and} \qquad RMSD_r^{U,e,\nu} = \frac{\left\|r^{U,src,\nu}\right\|_2}{\sqrt{K}}, \tag{32}$$

and the dual RMSDs of networks and units as

$$RMSD_s^{N,e,\nu} = \frac{\left\|s^{N,src,\nu}\right\|_2}{\sqrt{K}}, \qquad \text{and} \qquad RMSD_s^{U,e,\nu} = \frac{\left\|s^{U,src,\nu}\right\|_2}{\sqrt{K}}. \tag{33}$$

[16] Recall that $\left(\boldsymbol{\psi}_{n,k}^{N,src}\right)^{\nu+1} = \left(\boldsymbol{\psi}_{k,n}^{N,dest}\right)^{\nu+1}$ and $\left(\boldsymbol{\psi}_{i,k}^{U,src}\right)^{\nu+1} = \left(\boldsymbol{\psi}_{k,i}^{U,dest}\right)^{\nu+1}$ hold.

E. Cross-sectoral energy system model

To model the cross-sectoral and inter-temporal coupling of subproblems of a multitude of autonomous agents in the electricity and heat sector, key elements of the Cellular Energy System Model (CESM) presented in Schinke-Nendza et al. (2024b) are used, omitting some of its details regarding specific technologies (e.g., the hydrogen sector or residential power-to-heat applications). The CESM uses an linear programming (LP) formulation of a multi-energy system based on the following assumptions:

- All market participants are price takers, offering at their marginal production costs. As a consequence, the electricity market is competitive, while heat systems are operated in a cost-minimizing way.
- The modeling approach focuses on the spot energy market and network operation. Reserves and ancillary services are disregarded.
- A linear approximation neglecting losses is used, to model the AC-side of the electricity network. HVDC transmission lines are neglected in this study.

In the present paper, the modeling of the heat sector focuses on district heating networks exclusively. We denote these district heat networks in the following as heat regions, where the CESM adopts the approach introduced in Felten (2020) for modeling purposes. Note that in the following, variables and indices are used differently than in the front part of the paper.

E.1. Objective function

The objective function minimizes variable operational costs $C^{op}_{k,t}$ and start-up costs $C^{up}_{k,t}$ over time-steps $t \in \mathcal{T}$

$$\min \sum_{t \in \mathcal{T}} \left[\sum_{k \in \mathcal{K}_G} \left(C^{op}_{k,t} + C^{up}_{k,t} \right) + \sum_{n \in \mathcal{N}} C^{el,D}_{n,t} + \sum_{r \in \mathcal{R}} C^{h,D}_{r,t} \right], \quad (34)$$

with $k \in \mathcal{K}_G$ indicating all generation and supply units across all sectors (i.e. $\mathcal{K}_G = \mathcal{K}_{G,el} \cup \mathcal{K}_{G,h}$), while $C^{el,s}_{n,t}$ and $C^{h,s}_{r,t}$ are the costs of load shedding at electricity nodes $n \in \mathcal{N}$ and in heat regions $r \in \mathcal{R}$. With this formulation, infeasibilities are avoided, while load-shedding variables indicate a lack of security of supply.

E.2. Energy balances

For the *electricity network*, the nodal energy balances can be written as

$$\sum_{k \in \mathcal{K}_{G,el}(n)} p_{k,t}^{G,el} - \sum_{k \in \mathcal{K}_{PtH}(n)} p_{k,t}^{PtH} - p_{n,t}^{D} = p_{n,t}^{Ex}, \quad \forall n \in \mathcal{N}, t \in \mathcal{T}, \tag{35}$$

where $p_{k,t}^{G}$ is the electricity generation of units $k \in \mathcal{K}_{G,el}(n)$ located at node $n \in \mathcal{N}$ (with $\mathcal{K}_{G,el} = \mathcal{K}_{C} \cup \mathcal{K}_{CHP} \cup \mathcal{K}_{RES}$), $p_{k,t}^{PtH}$ is the electricity consumption of PtH units, $p_{n,t}^{D}$ is the residential and industrial electricity demand, and $p_{n,t}^{Ex}$ is the nodal net power injection transported across AC-lines.

In terms of the *district heating sector*, local networks are considered as heat regions. For each region $r \in \mathcal{R}$ and time-step $t \in \mathcal{T}$, the heat generation must be equal the heat demand $\dot{q}_{r,t}^{D}$

$$\sum_{k \in \mathcal{K}_{CHP}(r)} \dot{q}_{k,t}^{CHP} + \sum_{k \in \mathcal{K}_{PtH}(r)} \dot{q}_{k,t}^{PtH} + \sum_{k \in \mathcal{K}_{G,h}} \dot{q}_{k,t}^{G,h} + \dot{q}_{r,t}^{h,s} = \dot{q}_{r,t}^{D}, \tag{36}$$

where $\dot{q}_{k,t}^{G,CHP}$ is the heat supply of CHP units, $\dot{q}_{k,t}^{PtH}$ is the heat supply of PtH units (with constraints $\dot{q}_{k,t}^{PtH} = \epsilon_{k,t} \cdot p_{k,t}^{PtH}$ and $\dot{q}_{k,t}^{PtH} \leq \dot{q}_{k}^{PtH,+}$), $\dot{q}_{k,t}^{G,h}$ is the heat supply of heat-only plants. Constraints within district heating networks are disregarded to limit the overall problem size.

E.3. Electricity and heat demand

Regarding the shedding of electricity and heat demands, the value of lost load (VOLL) is used as a reference to determine costs. For a node $\in \mathcal{N}$ in a electricity network, the costs $C_{n,t}^{el,D}$ of residential and industrial electricity demand follow as

$$C_{n,t}^{el,D} = c^{el,VOLL} \left(p_{n,t}^{D+} - p_{n,t}^{D} \right) \Delta t \qquad \forall n \in \mathcal{N}, t \in \mathcal{T}. \tag{37}$$

For district heating networks, the costs of uncovered load $C_{r,t}^{h,D}$ in region $r \in \mathcal{R}$ may similarly be determined as

$$C_{r,t}^{h,D} = c^{h,VOLL} \left(\dot{q}_{r,t}^{D+} - \dot{q}_{r,t}^{D} \right) \Delta t \qquad \forall r \in \mathcal{R}, t \in \mathcal{T}. \tag{38}$$

E.4. Power transmission

Regarding the transmission of electricity across AC elements, a linear approximation is used (i.e., a DC-power flow) neglecting losses. The power flow $p_{m,t}^{AC,F}$ across a line $m \in \mathcal{M}_{AC}$ is then defined by

$$\sum_{l \in \mathcal{N}} \phi^N_{n,l} \cdot \theta_{l,t} = p^{Ex}_{n,t}, \qquad \forall n \in \mathcal{N}, t \in \mathcal{T}, \quad (39)$$

$$\sum_{n \in \mathcal{N}} \phi^L_{m,n} \cdot \theta_{n,t} = p^{AC,F}_{m,t}, \qquad \forall m \in \mathcal{M}_{AC}, t \in \mathcal{T}, \quad (40)$$

where $\theta_{n,t}$ is the voltage angle, while $\phi^N_{n,l}$ and $\phi^L_{m,n}$ are the elements of the nodal and line-related aggregated susceptance matrices. The power flow is limited by the maximum line capacity $p^{AC,+}_m$ in both directions

$$-p^{AC,+}_m \leq p^{AC,F}_{m,t} \leq p^{AC,+}_m, \qquad \forall m \in \mathcal{M}_{AC}, t \in \mathcal{T}. \quad (41)$$

E.5. Thermal power plants

For thermal power plants, i.e., notably methane-fueled GFPPs, a linear relaxation of the unit commitment problem is used to cope with operational limits. For units $k \in \mathcal{K}_C$, the operational constraints follow as

$$C^{C,op}_{k,t} = c^{C,op}_k \left[h^{op}_k p^C_{k,t} + (h^0_k - h^{op}_k) r^C_k p^C_k \right], \qquad \forall t \in \mathcal{T}, \quad (42)$$

$$C^{C,up}_{k,t} = c^{C,up}_k p^{C,up}_{k,t}, \qquad \forall t \in \mathcal{T}, \quad (43)$$

$$p^C_{k,t} \leq p^{C,onl}_{k,t} \leq p^{C,+}_k, \qquad \forall t \in \mathcal{T}, \quad (44)$$

$$p^{C,onl}_{k,t} - p^{C,onl}_{k,t-1} \leq p^{C,up}_{k,t}, \qquad \forall t \in \mathcal{T} \setminus \{t_1\} \quad (45)$$

$$r^C_k p^{C,onl}_{k,t} \leq p^C_{k,t}, \qquad \forall t \in \mathcal{T}, \quad (46)$$

$$0 \leq p^C_{k,t} \leq p^{C,+}_k, \qquad \forall t \in \mathcal{T}, \quad (47)$$

where $p^C_{k,t}$ is the power generation, $p^{C,up}_{k,t}$ is the start-up capacity, $p^{C,onl}_{k,t}$ the online capacity (an auxiliary variable of the linearly relaxed unit commitment problem), $r^C_k = p^{C,-}_k / p^{C,+}_k$ the minimum load factor, with heat rates $h^0_k = h^-_k$ and $h^{op}_k = (h^+_k - h^-_k r^C_k)/(1 - r^C_k)$.[17]

[17] Here, h^-_k and h^+_k are the inverse of the efficiencies at the minimal operating output $p^{C,-}_k$ and the maximum output $p^{C,+}_k$.

E.6. Combined heat and power plants

Regarding CHP plants, the power supply is modeled as given by constraints (42)-(47). In terms of the heat supply, back-pressure turbines $\mathcal{K}_{BP}$ and extraction-condensing turbines $\mathcal{K}_{EC}$ can be distinguished, with $\mathcal{K}_{CHP} = \mathcal{K}_{BP} \cup \mathcal{K}_{EC}$. The heat-related constraints follow to

$$0 \leq \dot{q}_{k,t}^{CHP} \leq \dot{q}_{k,t}^{CHP,+}, \qquad \forall k \in \mathcal{K}_{CHP}, t \in \mathcal{T}, \quad (48)$$

$$p_{k,t}^{CHP} = \delta_k^{CHP} \dot{q}_{k,t}^{CHP}, \qquad \forall k \in \mathcal{K}_{BP}, t \in \mathcal{T}, \quad (49)$$

$$p_{k,t}^{CHP} \geq \delta_k^{CHP} \dot{q}_{k,t}^{CHP}, \qquad \forall k \in \mathcal{K}_{EC}, t \in \mathcal{T}, \quad (50)$$

$$r_k^{CHP} p_{k,t}^{CHP,onl} \leq p_{k,t}^{CHP} + \gamma_k^{CHP} \dot{q}_{k,t}^{CHP} \leq p_{k,t}^{CHP,onl}, \qquad \forall k \in \mathcal{K}_{EC}, t \in \mathcal{T}, \quad (51)$$

where $\dot{q}_{k,t}^{CHP}$ is the heat supply, $\dot{q}_{k,t}^{CHP,+}$ is the maximum heat supply, δ_k^{CHP} is the power-to-heat ratio, and γ_k^{CHP} is the power-loss coefficient.

E.7. Renewable energy sources

Solar, wind, and run-of-the-river hydro power plants are considered regarding renewable power supply. These technologies are assumed to come along with zero marginal cost and modeled based on an exogenous time series of the maximum power infeed $p_{k,t}^{RES,+}$

$$0 \leq p_{k,t}^{RES} \leq p_{k,t}^{RES,+}, \qquad \forall k \in \mathcal{K}_{RES}, t \in \mathcal{T}. \quad (52)$$

Correspondence

Aiko Schinke-Nendza, M.Sc.

Research Associate

House of Energy Markets and Finance

University of Duisburg-Essen, Germany

Universitätsstr. 12, 45117

Tel. +49 201 183-5625

Fax +49 201 183-2703

E-Mail aiko.schinke-nendza@uni-due.de